Supplementary information for

Rates of pyruvate carboxylase, glutamate and GABA neurotransmitter cycling, and glucose oxidation in multiple brain regions of the awake rat using a combination of [2-^{13}C]/[1-^{13}C]glucose infusion and ^{1}H-[^{13}C]NMR *ex vivo*

Laura M McNair[1,#], Graeme F Mason[2,3,4], Golam M I Chowdhury[3], Lihong Jiang[2], Xiaoxian Ma[2], Douglas L Rothman[2,4], Helle S Waagepetersen[1], Kevin L Behar[3,#]

[1]Department of Drug Design and Pharmacology, Faculty of Health and Medical Sciences, University of Copenhagen, Copenhagen, Denmark; [2]Department of Radiology and Biomedical Imaging, Magnetic Resonance Research Center, Yale University School of Medicine, New Haven, Connecticut, USA; [3]Department of Psychiatry, Yale University School of Medicine, New Haven, Connecticut, USA; [4]Department of Biomedical Engineering, Yale University, New Haven, Connecticut, USA;

[#]Correspondence: Laura M McNair, Jagtvej 160, 2100 Copenhagen Ø, Denmark; +45 29725647; laura.mcnair@sund.ku.dk; @UCPH_health or Kevin L Behar, Yale University, MRRC TAC N151, 300 Cedar St, PO Box 208043, New Haven, Connecticut 06520, USA; 203-481-4714; kevin.behar@yale.edu

Supplementary information for Rates of pyruvate carboxylase, glutamate and GABA neurotransmitter cycling, and glucose oxidation in multiple brain regions of the awake rat using a combination of [2-^{13}C]/[1-^{13}C]glucose infusion and ^{1}H-[^{13}C]NMR *ex vivo,* by LM McNair *et al.* 2021, JCBFM

Supplementary information

Table S1. Mass and isotope balance equations, combination pools, values of rates and values of pool concentrations for the metabolic calculations following fitting of cerebral cortical data.

Mass Balance:

$dBrain\_Glucose2/dt = Vglc\_in2 - [CMRglc(ox) + Vglc\_out2]$

$dBrain\_Glucose1/dt = Vglc\_in1 - [CMRglc(ox) + Vglc\_out1]$

$dL1/dt = dL2/dt = 2CMRglc(ox) - [Vpc + Vpdh_A + Vpdh_{GA} + Vpdh_N]$

$dAcCoAA1/dt = dAcCoAA2/dt = Vpdh_A + Vdil_{A\_in} - [Vtca_A]$

$dKGA1/dt = dKGA2/dt = Vx_{GluKGA} + Vtca_A - [Vtca_{ANet} + Vx_{KGGluA}]$

$dKGN1/dt = dKGN2/dt = Vx_{GluKGN} + Vdil_N + Vpdh_N - [Vx_{KGGluN} + Vtca_N]$

$dKGGA1/dt = dKGGA2/dt = Vx_{GluKGGA} + Vpdh_{GA} + Vdil_{GA} - [Vtca_{GANet} + Vx_{KGGluGA}]$

$dGln1/dt = dGln2/dt = Vgln + Vdil_{Gln} - [Vefflux + Vcyc_{GluGln} + Vcyc_{GABAGln}]$

$dGluN1/dt = dGluN2/dt = Vcyc_{GluGln} + Vx_{KGGluN} - [Vcyc_{GluGln} + Vx_{GluKGN}]$

$dGluA1/dt = dGluA2/dt = Vcyc_{GluGln} + Vx_{KGGluA} - [Vgln + Vx_{GluKGA}]$

$dGluGA1/dt = dGluGA2/dt = Vcyc_{GABAGln} + Vx_{KGGluGA} - [Vgad + Vx_{GluKGGA}]$

$dGABA1/dt = dGABA2/dt = Vgad - [Vshunt + Vcyc_{GABAGln}]$

$dFumA1/dt = dFumA2/dt = Vcyc_{GABAGln} + Vtca_{ANet} + Vsc - Vtca_{ANetprime}$

$dOAAN1/dt = dOAAN2/dt = Vx_{AspOAAN} + Vtca_N - [Vx_{OAAAspN} + Vtca_N]$

$dOAAA1/dt = dOAAA2/dt = Vx_{AspOAAA} + Vpc + Vtca_{ANetprime} - [Vx_{OAAAspA} + Vtca_A + Vsc]$

$dOAAGA1/dt = dOAAGA2/dt = Vtca_{GANet} + Vshunt + Vx_{AspOAAGA} - [Vtca_{GA} + Vx_{OAAAspGA}]$

$dAspN1/dt = dAspN2/dt = Vx_{OAAAspN} - Vx_{AspOAAN}$

$dAspA1/dt = dAspA2/dt = Vx_{OAAAspA} - Vx_{AspOAAA}$

$dAspGA1/dt = dAspGA2/dt = Vx_{OAAAspGA} - Vx_{AspOAAGA}$

Isotope Balance related to [1-^{13}C]glucose:

$dBrain\_Glucose1_1/dt = Vglc\_in1(Blood\_Glucose1_1/Blood\_Glucose1) - [CMRglc(ox) + Vglc\_out1](Brain\_Glucose1_1/Brain\_Glucose1)$

$dP1_3/dt = CMRglc(ox)(Brain\_Glucose1_1/Brain\_Glucose1) - [Vpc + Vpdh_A + Vpdh_{GA} + Vpdh_N](P1_3/P1)$

$dAcCoAA1_2/dt = VpdhA(P1_3/P1) + Vdil_{A\_in}(0) - [Vtca_A](AcCoAA1_2/AcCoAA1)$

$dKGN1_2/dt = Vx_{GluKGN}(GluN1_2/GluN1) + Vtca_N(OAAN1_3/OAAN1) - [Vx_{KGGluN} + Vtca_N](KGN1_2/KGN1)$

$dKGGA1_2/dt = Vx_{GluKGGA}(GluGA1_2/GluGA1) + Vtca_{GA}(OAAGA1_3/OAAGA1) - [Vtca_{GANet} + Vx_{KGGluGA}](KGGA1_2/KGGA1)$

$dKGA1_2/dt = Vx_{GluKGA}(GluA1_2/GluA1) + Vtca_A(OAAA1_3/OAAA1) - [Vtca_{ANet} + Vx_{KGGluA}](KGA1_2/KGA1)$

$dKGN1_3/dt = Vx_{GluKGN}(GluN1_3/GluN1) + Vtca_N(OAAN1_2/OAAN1) - [Vx_{KGGluN} + Vtca_N](KGN1_3/KGN1)$

$dKGGA1_3/dt = Vx_{GluKGGA}(GluGA1_3/GluGA1) + Vtca_{GA}(OAAGA1_2/OAAGA1) - [Vtca_{GANet} + Vx_{KGGluGA}](KGGA1_3/KGGA1)$

$dKGA1_3/dt = Vx_{GluKGA}(GluA1_3/GluA1) + Vtca_A(OAAA1_2/OAAA1) - [Vtca_{ANet} + Vx_{KGGluA}](KGA1_3/KGA1)$

$dKGN1_4/dt = Vx_{GluKGN}(GluN1_4/GluN1) + Vdil_N(0) + Vpdh_N(P1_3/P1) - [Vx_{KGGluN} + Vtca_N](KGN1_4/KGN1)$

$dKGGA1_4/dt = Vpdh_{GA}(P1_3/P1) + Vx_{GluKGGA}(GluGA1_4/GluGA1) + Vdil_{GA}(0) - [Vtca_{GANet} + Vx_{KGGluGA}](KGGA1_4/KGGA1)$

$dKGA1_4/dt = Vx_{GluKGA}(GluA1_4/GluA1) + Vtca_A(AcCoAA1_2/AcCoAA1) - [Vtca_{ANet} + Vx_{KGGluA}](KGA1_4/KGA1)$

$dGluN1_2/dt = Vcyc_{GluGln}(Gln1_2/Gln1) + Vx_{KGGluN}(KGN1_2/KGN1) - [Vcyc_{GluGln} + Vx_{GluKGN}](GluN1_2/GluN1)$

$dGluGA1_2/dt = Vcyc_{GABAGln}(Gln1_2/Gln1) + Vx_{KGGluGA}(KGGA1_2/KGGA1) - [Vgad + Vx_{GluKGGA}](GluGA1_2/GluGA1)$

$dGluA1_2/dt = Vx_{KGGluA}(KGA1_2/KGA1) + Vcyc_{GluGln}(GluN1_2/GluN1) - [Vgln + Vx_{GluKGA}](GluA1_2/GluA1)$

$dGluN1_3/dt = Vcyc_{GluGln}(Gln1_3/Gln1) + Vx_{KGGluN}(KGN1_3/KGN1) - [Vcyc_{GluGln} + Vx_{GluKGN}](GluN1_3/GluN1)$

$dGluGA1_3/dt = Vcyc_{GABAGln}(Gln1_3/Gln1) + Vx_{KGGluGA}(KGGA1_3/KGGA1) - [Vgad + Vx_{GluKGGA}](GluGA1_3/GluGA1)$

$dGluA1_3/dt = Vx_{KGGluA}(KGA1_3/KGA1) + Vcyc_{GluGln}(GluN1_3/GluN1) - [Vgln + Vx_{GluKGA}](GluA1_3/GluA1)$

$dGluN1_4/dt = Vcyc_{GluGln}(Gln1_4/Gln1) + Vx_{KGGluN}(KGN1_4/KGN1) - [Vcyc_{GluGln} + Vx_{GluKGN}](GluN1_4/GluN1)$

$dGluGA1_4/dt = Vcyc_{GABAGln}(Gln1_4/Gln1) + Vx_{KGGluGA}(KGGA1_4/KGGA1) - [Vgad + Vx_{GluKGGA}](GluGA1_4/GluGA1)$

$dGluA1_4/dt = Vcyc_{GluGln}(GluN1_4/GluN1) + Vx_{KGGluA}(KGA1_4/KGA1) - [Vgln + Vx_{GluKGA}](GluA1_4/GluA1)$

$dGln1_2/dt = Vdil_{Gln}(0) + Vgln(GluA1_2/GluA1) - [Vefflux + Vcyc_{GluGln} + Vcyc_{GABAGln}](Gln1_2/Gln1)$

$dGln1_3/dt = Vgln(GluA1_3/GluA1) + Vdil_{Gln}(0) - [Vefflux + Vcyc_{GluGln} + Vcyc_{GABAGln}](Gln1_3/Gln1)$

$dGln1_4/dt = Vgln(GluA1_4/GluA1) + Vdil_{Gln}(0) - [Vefflux + Vcyc_{GluGln} + Vcyc_{GABAGln}](Gln1_4/Gln1)$

$dGABA1_2/dt = Vgad(GluGA1_4/GluGA1) - [Vshunt + Vcyc_{GABAGln}](GABA1_2/GABA1)$

$dGABA1_3/dt = Vgad(GluGA1_3/GluGA1) - [Vshunt + Vcyc_{GABAGln}](GABA1_3/GABA1)$

$dGABA1_4/dt = Vgad(GluGA1_2/GluGA1) - [Vshunt + Vcyc_{GABAGln}](GABA1_4/GABA1)$

$dFumA1_2/dt = 0.5Vcyc_{GABAGln}(GABA1_2/GABA1) + 0.5Vcyc_{GABAGln}(GABA1_3/GABA1) + 0.5Vtca_{ANet}(KGA1_4/KGA1) + 0.5Vtca_{ANet}(KGA1_3/KGA1) + 0.5Vsc(OAAA1_2/OAAA1) + 0.5Vsc(OAAA1_3/OAAA1) - Vtca_{ANetprime}(FumA1_2/FumA1)$

$dFumA1_3/dt = 0.5Vcyc_{GABAGln}(GABA1_2/GABA1) + 0.5Vcyc_{GABAGln}(GABA1_3/GABA1) + 0.5Vtca_{ANet}(KGA1_4/KGA1) + 0.5Vtca_{ANet}(KGA1_3/KGA1) + 0.5Vsc(OAAA1_2/OAAA1) + 0.5Vsc(OAAA1_3/OAAA1) - Vtca_{ANetprime}(FumA1_3/FumA1)$

$dOAAN1_2/dt = Vx_{AspOAAN}(AspN1_2/AspN1) + 0.5Vtca_N(KGN1_4/KGN1) + 0.5Vtca_N(KGN1_3/KGN1) - [Vx_{OAAAspN} + Vtca_N](OAAN1_2/OAAN1)$

$dOAAGA1_2/dt = 0.5Vtca_{GANet}(KGGA1_3/KGGA1) + 0.5Vtca_{GANet}(KGGA1_4/KGGA1) + 0.5Vshunt(GABA1_2/GABA1) + 0.5Vshunt(GABA1_3/GABA1) + Vx_{AspOAAGA}(AspGA1_2/AspGA1) - [Vtca_{GABA} + Vx_{OAAAspGA}](OAAGA1_2/OAAGA1)$

$dOAAA1_2/dt = Vx_{AspOAAA}(AspA1_2/AspA1) + Vpc(0) + Vtca_{ANetprime}(FumA1_2/FumA1) - [Vx_{OAAAspA} + Vtca_A + Vsc](OAAA1_2/OAAA1)$

$dOAAN1_3/dt = Vx_{AspOAAN}(AspN1_3/AspN1) + 0.5Vtca_N(KGN1_3/KGN1) + 0.5Vtca_N(KGN1_4/KGN1) - [Vx_{OAAAspN} + Vtca_N](OAAN1_3/OAAN1)$

$dOAAGA1_3/dt = 0.5Vtca_{GANet}(KGGA1_4/KGGA1) + 0.5Vtca_{GANet}(KGGA1_3/KGGA1) + 0.5Vshunt(GABA1_2/GABA1) + 0.5Vshunt(GABA1_3/GABA1) + Vx_{AspOAAGA}(AspGA1_3/AspGA1) - [Vtca_{GABA} + Vx_{OAAAspGA}](OAAGA1_3/OAAGA1)$

$dOAAA1_3/dt = Vx_{AspOAAA}(AspA1_3/AspA1) + Vpc(P1_3/P1) + Vtca_{ANetprime}(FumA1_3/FumA1) - [Vx_{OAAAspA} + Vtca_A + Vsc](OAAA1_3/OAAA1)$

$dAspN1_2/dt = Vx_{OAAAspN}(OAAN1_2/OAAN1) - Vx_{AspOAAN}(AspN1_2/AspN1)$

$dAspGA1_2/dt = Vx_{OAAAspGA}(OAAGA1_2/OAAGA1) - Vx_{AspOAAGA}(AspGA1_2/AspGA1)$

$dAspA1_2/dt = Vx_{OAAAspA}(OAAA1_2/OAAA1) - Vx_{AspOAAA}(AspA1_2/AspA1)$

$dAspN1_3/dt = Vx_{OAAAspN}(OAAN1_3/OAAN1) - Vx_{AspOAAN}(AspN1_3/AspN1)$

$dAspGA1_3/dt = Vx_{OAAAspGA}(OAAGA1_3/OAAGA1) - Vx_{AspOAAGA}(AspGA1_3/AspGA1)$

$dAspA1_3/dt = Vx_{OAAAspA}(OAAA1_3/OAAA1) - Vx_{AspOAAA}(AspA1_3/AspA1)$

Isotope Balance related to [2-^{13}C]glucose:

$dBrain\_Glucose2_2/dt = Vglc\_in2(Blood\_Glucose2_2/Blood\_Glucose2) - [CMRglc(ox) + Vglc\_out2](Brain\_Glucose2_2/Brain\_Glucose2)$

$dBrain\_Glucose2_{1,6}/dt = Vglc\_in2(Blood\_Glucose2_{1,6}/Blood\_Glucose2) - [CMRglc(ox) + Vglc\_out2](Brain\_Glucose2_{1,6}/Brain\_Glucose2)$

$dP2_2/dt = CMRglc(ox)(Brain\_Glucose2_2/Brain\_Glucose2) - [Vpc + VpdhA + Vpdh_{GA} + Vpdh_N](P2_2/P2)$

$dP2_3/dt = 2CMRglc(ox)(Brain\_Glucose2_{1,6}/Brain\_Glucose2) - [Vpc + VpdhA + Vpdh_{GA} + Vpdh_N](P2_3/P2)$

$dAcCoAA2_1/dt = VpdhA(P2_2/P2)) + Vdil_{A\_in}(0) - [Vtca_A](AcCoAA2_1/AcCoAA2)$

$dAcCoAA2_2/dt = VpdhA(P2_3/P2) + Vdil_{A\_in}(0) - [Vtca_A](AcCoAA2_2/AcCoAA2)$

$dKGN2_2/dt = Vx_{GluKGN}(GluN2_2/GluN2) + Vtca_N(OAAN2_3/OAAN2) - [Vtca_N + Vx_{KGGluN}](KGN2_2/KGN2)$

$dKGGA2_2/dt = Vx_{GluKGGA}(GluGA2_2/GluGA2) + Vtca_{GA}(OAAGA2_3/OAAGA2) - [Vtca_{GANet} + Vx_{KGGluGA}](KGGA2_2/KGGA2)$

$dKGA2_2/dt = Vx_{GluKGA}(GluA2_2/GluA2) + Vtca_A(OAAA2_3/OAAA2) - [Vtca_{ANet} + Vx_{KGGluA}](KGA2_2/KGA2)$

$dKGA2_4/dt = Vtca_A(AcCoAA2_2/AcCoAA2) + Vx_{GluKGA}(GluA2_4/GluA2) - [Vtca_{ANet} + Vx_{KGGluA}](KGA2_4/KGA2)$

$dKGN2_3/dt = Vx_{GluKGN}(GluN2_3/GluN2) + Vtca_N(OAAN2_2/OAAN2) - [Vtca_N + Vx_{KGGluN}](KGN2_3/KGN2)$

$dKGGA2_3/dt = Vx_{GluKGGA}(GluGA2_3/GluGA2) + Vtca_{GA}(OAAGA2_2/OAAGA2) - [Vtca_{GANet} + Vx_{KGGluGA}](KGGA2_3/KGGA2)$

$dKGN2_4/dt = Vx_{GluKGN}(GluN2_4/GluN2) + Vpdh_N(P2_3/P2) + Vdil_N(0) - [Vtca_N + Vx_{KGGluN}](KGN2_4/KGN2)$

$dKGGA2_4/dt = Vx_{GluKGGA}(GluGA2_4/GluGA2) + Vpdh_{GA}(P2_3/P2) + Vdil_{GA}(0) - [Vtca_{GANet} + Vx_{KGGluGA}](KGGA2_4/KGGA2)$

$dKGA2_3/dt = Vx_{GluKGA}(GluA2_3/GluA2) + Vtca_A(OAAA2_2/OAAA2) - [Vtca_{ANet} + Vx_{KGGluA}](KGA2_3/KGA2)$

$dGluN2_2/dt = Vcyc_{GluGln}(Gln2_2/Gln2) + Vx_{KGGluN}(KGN2_2/KGN2) - [Vcyc_{GluGln} + Vx_{GluKGN}](GluN2_2/GluN2)$

$dGluGA2_2/dt = Vcyc_{GABAGln}(Gln2_2/Gln2) + Vx_{KGGluGA}(KGGA2_2/KGGA2) - [Vgad + Vx_{GluKGGA}](GluGA2_2/GluGA2)$

$dGluA2_2/dt = Vcyc_{GluGln}\ (GluN2_2/GluN2) + Vx_{KGGluA}(KGA2_2/KGA2) - [Vgln + Vx_{GluKGA}](GluA2_2/GluA2)$

$dGluN2_3/dt = Vcyc_{GluGln}(Gln2_3/Gln2) + Vx_{KGGluN}(KGN2_3/KGN2) - [Vcyc_{GluGln} + Vx_{GluKGN}](GluN2_3/GluN2)$

$dGluGA2_3/dt = Vcyc_{GABAGln}(Gln2_3/Gln2) + Vx_{KGGluGA}(KGGA2_3/KGGA2) - [Vgad + Vx_{GluKGGA}](GluGA2_3/GluGA2)$

$dGluA2_3/dt = Vcyc_{GluGln}(GluN2_3/GluN2) + VxKGGluA(KGA2_3/KGA2) - [Vgln + Vx_{GluKGA}](GluA2_3/GluA2)$

$dGluN2_4/dt = Vcyc_{GluGln}(Gln2_4/Gln2) + Vx_{KGGluN}(KGN2_4/KGN2) - [Vcyc_{GluGln} + Vx_{GluKGN}](GluN2_4/GluN2)$

$dGluGA2_4/dt = Vcyc_{GABAGln}(Gln2_4/Gln2) + Vx_{KGGluGA}(KGGA2_4/KGGA2) - [Vgad + Vx_{GluKGGA}](GluGA2_4/GluGA2)$

$dGluA2_4/dt = Vcyc_{GluGln}(GluN2_4/GluN2) + Vx_{KGGluA}(KGA2_4/KGA2) - [Vgln + Vx_{GluKGA}](GluA2_4/GluA2)$

$dGln2_2/dt = Vgln(GluA2_2/GluA2) + Vdil_{Gln}(0) - [Vcyc_{GluGln} + Vcyc_{GABAGln} + Vefflux](Gln2_2/Gln2)$

$dGln2_3/dt = Vgln(GluA2_3/GluA2) + Vdil_{Gln}(0) - [Vcyc_{GluGln} + Vcyc_{GABAGln} + Vefflux](Gln2_3/Gln2)$

$dGln2_4/dt = Vgln(GluA2_4/GluA2) + Vdil_{Gln}(0) - [Vcyc_{GluGln} + Vcyc_{GABAGln} + Vefflux](Gln2_4/Gln2)$

$dGABA2_2/dt = Vgad(GluGA2_4/GluGA2) - [Vcyc_{GABAGln} + Vshunt](GABA2_2/GABA2)$

$dGABA2_3/dt = Vgad(GluGA2_3/GluGA2) - [Vcyc_{GABAGln} + Vshunt](GABA2_3/GABA2)$

$dGABA2_4/dt = Vgad(GluGA2_2/GluGA2) - [Vcyc_{GABAGln} + Vshunt](GABA2_4/GABA2)$

$dFumA2_2/dt = 0.5Vcyc_{GABAGln}(GABA2_2/GABA2) + 0.5Vcyc_{GABAGln}(GABA2_3/GABA2) + 0.5Vtca_{ANet}(KGA2_4/KGA2) + 0.5Vtca_{ANet}(KGA2_3/KGA2) 0+ 0.5Vsc(OAAA2_2/OAAA2) + 0.5Vsc(OAAA2_3/OAAA2) - Vtca_{ANetprime}(FumA2_2/FumA2)$

$dFumA2_3/dt = 0.5Vcyc_{GABAGln}(GABA2_2/GABA2) + 0.5Vcyc_{GABAGln}(GABA2_3/GABA2) + 0.5Vtca_{ANet}(KGA2_4/KGA2) + 0.5Vtca_{ANet}(KGA2_3/KGA2) 0+ 0.5Vsc(OAAA2_2/OAAA2) + 0.5Vsc(OAAA2_3/OAAA2) - Vtca_{ANetprime}(FumA2_3/FumA2)$

$dAspN2_2/dt = Vx_{OAAAspN}(OAAN2_2/OAAN2) - Vx_{AspOAAN}(AspN2_2/AspN2)$

$dAspGA2_2/dt = Vx_{OAAAspGA}(OAAGA2_2/OAAGA2) - Vx_{AspOAAGA}(AspGA2_2/AspGA2)$

$dAspA2_2/dt = Vx_{OAAAspA}(OAAA2_2/OAAA2) - Vx_{AspOAAA}(AspA2_2/AspA2)$

$dAspN2_3/dt = Vx_{OAAAspN}(OAAN2_3/OAAN2) - Vx_{AspOAAN}(AspN2_3/AspN2)$

$dAspGA2_3/dt = VxOAAAspGA(OAAGA2_3/OAAGA2) - VxAspOAAGA(AspGA2_3/AspGA2)$

$dAspA2_3/dt = Vx_{OAAAspA}(OAAA2_3/OAAA2) - Vx_{AspOAAA}(AspA2_3/AspA2)$

$dOAAN2_2/dt = Vx_{AspOAAN}(AspN2_2/AspN2) + 0.5Vtca_N(KGN2_4/KGN2) + 0.5Vtca_N(KGN2_3/KGN2) - [Vtca_N + Vx_{OAAAspN}](OAAN2_2/OAAN2)$

$dOAAGA2_2/dt = Vx_{AspOAAGA}(AspGA2_2/AspGA2) + 0.5Vshunt(GABA2_2/GABA2) + 0.5Vshunt(GABA2_3/GABA2) + 0.5Vtca_{GANet}(KGGA2_4/KGGA2) + 0.5Vtca_{GANet}(KGGA2_3/KGGA2) - [Vtca_{GABA} + Vx_{OAAAspGA}](OAAGA2_2/OAAGA2)$

$dOAAA2_2/dt = Vx_{AspOAAA}(AspA2_2/AspA2) + Vtca_{ANetprime}(FumA2_2/FumA2) + Vpc(P2_2/P2) - [Vsc + Vtca_A + Vx_{OAAAspA}](OAAA2_2/OAAA2)$

$dOAAN2_3/dt = Vx_{AspOAAN}(AspN2_3/AspN2) + 0.5Vtca_N(KGN2_4/KGN2) + 0.5Vtca_N(KGN2_3/KGN2) - [Vtca_N + Vx_{OAAAspN}](OAAN2_3/OAAN2)$

$dOAAGA2_3/dt = Vx_{AspOAAGA}(AspGA2_3/AspGA2) + 0.5Vshunt(GABA2_2/GABA2) + 0.5Vshunt(GABA2_3/GABA2) + 0.5Vtca_{GANet}(KGGA2_4/KGGA2) + 0.5Vtca_{GANet}(KGGA2_3/KGGA2) - [Vtca_{GABA} + Vx_{OAAAspGA}](OAAGA2_3/OAAGA2)$

$dOAAA2_3/dt = Vx_{AspOAAA}(AspA2_3/AspA2) + Vtca_{ANetprime}(FumA2_3/FumA2) + Vpc(P2_3/P2) - [Vsc + Vtca_A + Vx_{OAAAspA}](OAAA2_3/OAAA2)$

Combination Pools:

GluTot1_C2 = sum of C2 labeled GluN1, GluGA1, and GluA1 from infusions with [1-^{13}C]glucose

GluTot1_C3 = sum of C3 labeled GluN1, GluGA1, and GluA1 from infusions with [1-^{13}C]glucose

GluTot1_C4 = sum of C4 labeled GluN1, GluGA1, and GluA1 from infusions with [1-^{13}C]glucose

GluTot2_C2 = sum of C2 labeled GluN2, GluGA2, and GluA2 from infusions with [2-^{13}C]glucose

GluTot2_C3 = sum of C3 labeled GluN2, GluGA2, and GluA2 from infusions with [2-^{13}C]glucose

GluTot2_C4 = sum of C4 labeled GluN2, GluGA2, and GluA2 from infusions with [2-^{13}C]glucose

AspTot1_C3 = sum of C3 labeled AspN1, AspGA1, and AspA1 from infusions with [1-^{13}C]glucose

AspTot1_C2 = sum of C2 labeled AspN1, AspGA1, and AspA1 from infusions with [1-^{13}C]glucose

Values of Rates (**iterated** rates in bold):

$CMRglc(ox) = (Vpdh_A+Vpdh_N+Vpdh_{GA}+Vpc)/2 = 0.802$ µmol/min/g; Rate of glucose oxidation

Km_in = 3.3 mM; Michaelis-Menten half-saturation constant for blood-brain glucose transport (Mason et al., 1992)

Km_out = Km_in*Vd = 2.541 µmol/g; Michaelis-Menten half-saturation constant for brain-blood glucose transport

$PercVtca_{GANet}$ = 84.316; The amount of the GABAergic TCA cycle (as percentage) that continues beyond KG through OAA. (**Iterated**)

R_AspA_AspTot = 0.1; Fraction Asp in astroglia

R_AspGA_AspTot = 0.02; Fraction Asp in GABAergic neurons

R_AspN_AspTot = 1-R_AspGA_AspTot-R_AspA_AspTot = 0.88; Fraction Asp in glutamatergic neurons

$R\_Vcyc_{GluGln}\_Vtca_N = Vcyc_{GluGln}/Vtca_N = 0.552$; Ratio between Vcyc(Glu/Gln) and $Vtca_N$

$R\_Vdil_{Gln}\_Vgln$ = 0.26997; Ratio between $Vdil_{Gln}$ and Vgln (**Iterated**)

$R\_VscVtca_A = 0.37$; Ratio between Vsc and $Vtca_A$ calculated from rates reported by Öz et al. (2004)

$Vcyc_{GluGln}$ = 0.700 µmol/min/g; Rate of glutamate-glutamine cycling (**Iterated**)

$Vcyc_{GABAGln}$ = 0.109 µmol/min/g; Rate of GABA-glutamine cycling (**Iterated**)

Vd = 0.77 ml/g; Brain water space (Buschiazzo et al., 1970)

$Vdil_{A\_in}$ = 0.090 µmol/min/g; Rate of dilution in astroglia (**Iterated**)

$Vdil_{GA}$ = 0.090 µmol/min/g; Rate of dilution in GABAergic neurons (**Iterated**)

$Vdil_{Gln} = R\_Vdil_{Gln}\_Vgln*Vgln = 0.247$ µmol/min/g; Rate of diluting Gln exchanged from blood

$Vdil_N$ = 0.127 µmol/min/g; Rate of dilution in glutamatergic neurons (**Iterated**)

$Vefflux = Vpc+Vdil_{Gln} = 0.353$ µmol/min/g; Rate of loss of carbon from the astroglial TCA cycle via efflux of Gln from the brain, partly balanced by entry of glutamine from the blood, also at the rate $Vdil_{Gln}$

$Vgad = Vshunt+Vcyc_{GABAGln} = 0.159$ µmol/min/g; Rate of GABA synthesis through glutamate decarboxylase (GAD)

Vglc_in1 = Blood_Glucose1*Vmax_in/(Blood_Glucose1+Km_in+Brain_Glucose1/Vd) (time-varying); Rate of glucose entry into brain in the [1-^{13}C]glucose experiment.

Vglc_out1 = Brain_Glucose1*Vmax_out/(Blood_Glucose1*Vd+Km_out+Brain_Glucose1) (time-varying); Rate of glucose out of brain in the [1-^{13}C]glucose experiment.

Vglc_in2 = Blood_Glucose1*Vmax_in/(Blood_Glucose2+Km_in+Brain_Glucose2/Vd) (time-varying); Rate of glucose entry into brain in the [2-^{13}C]glucose experiment.

Vglc_out2 = Brain_Glucose1*Vmax_out/(Blood_Glucose2*Vd+Km_out+Brain_Glucose2) (time-varying); Rate of glucose out of brain in the [2-^{13}C]glucose experiment.

$Vgln = Vcyc_{GluGln}+Vcyc_{GABAGln}+Vpc = 0.915$ µmol/min/g; Rate of Gln synthesis

Vmax_in = 2.7*CMRglc(ox) = 2.165 µmol/min/g; Vmax for glucose flow from blood to brain

Vmax_out = Vmax_in = 2.165 µmol/min/g; Vmax for glucose flow from brain to blood

$Vpc = Vtca_A-Vtca_{ANet}-Vcyc_{GABAGln} = 0.106$ µmol/min/g; Rate of pyruvate carboxylase (PC)

$Vpdh_A$ = 0.126 µmol/min/g; Rate of pyruvate dehydrogenase (PDH) in astroglia (**Iterated**)

$Vpdh_{GA}$ = 0.229 µmol/min/g; Rate of pyruvate dehydrogenase (PDH) in GABAergic neurons (**Iterated**)

$Vpdh_N = Vtca_N - Vdil_N = 1.142$ µmol/min/g; Rate of pyruvate dehydrogenase (PDH) in glutamatergic neurons

$Vsc = R\_VscVtca_A*Vtca_A = 0.080$ µmol/min/g; Rate of scrambling (modified from Oz et al., 2004)

$Vshunt = Vtca_{GA}-Vtca_{GANet} = 0.050$ µmol/min/g; Rate of the GABA shunt, i.e. GABA degradation in the GABAergic neuron

$Vtca_A = Vpdh_A+Vdil_{A\_in} = 0.217$ µmol/min/g; Rate of astroglial TCA cycle flow from citric acid through KG

$Vtca_{ANet}$ = 0.001 µmol/min/g; Rate of astroglial TCA cycle flow from KG to succinate (**Iterated**)

$Vtca_{ANetprime} = Vcyc_{GABAGln}+Vtca_{ANet}+Vsc = 0.190$ µmol/min/g; Rate of astroglial TCA cycle flow from succinate to OAA

$Vtca_{GA} = Vpdh_{GA}+Vdil_{GA} = 0.320$µmol/min/g; Rate of GABAergic neuronal TCA cycle flow from citric acid through KG

$Vtca_{GANet} = Vtca_{GA}*PercVtca_{GANet}/100 = 0.270$ µmol/min/g; Rate of GABAergic neuronal TCA cycle flow from KG to succinate

$Vtca_N$ = 1.268 µmol/min/g; Rate of glutamatergic neuronal TCA cycle flow (**Iterated**)

$Vtca_{Tot} = Vtca_A+Vtca_{GA}+Vtca_N = 1.805$ µmol/min/g; Rate of total TCA cycle flux

$Vx_{AspOAAA} = Vx_{OAAAspA}$ = 1 µmol/min/g; Rate of exchange from Asp to OAA in astroglia

$Vx_{AspOAAGA} = Vx_{OAAAspGA}$ = 10 µmol/min/g; Rate of exchange from Asp to OAA in GABAergic neurons

$Vx_{AspOAAN} = Vx_{OAAAspN}$ = 11.854 µmol/min/g; Rate of exchange from Asp to OAA in glutamatergic neurons

Vx_{GluKGA} = 1 µmol/min/g; Rate of exchange from Glu to KG in astroglia, value unknown, sensitivity evaluated and found to be low (Supplemental Information)

$Vx_{GluKGGA}$ = 10 µmol/min/g; Rate of exchange from Glu to KG in GABAergic neurons, value unknown, sensitivity evaluated and found to be low (Supplemental Information)

Vx_{GluKGN} = 11.854 µmol/min/g; Rate of exchange from Glu to KG in glutamatergic neurons (**Iterated**)

$Vx_{KGGluA} = Vx_{GluKGA}$+Vgln-$Vcyc_{GluGln}$ = 1.215 µmol/min/g; Rate of exchange from KG to Glu in astroglia

$Vx_{KGGluGA} = Vx_{GluKGGA}$+Vgad-$Vcyc_{GABAGln}$ = 10.050 µmol/min/g; Rate of exchange from KG to Glu in GABAergic neurons

$Vx_{KGGluN} = Vx_{GluKGN}$ = 11.854 µmol/min/g; Rate of exchange from KG to Glu in glutamatergic neurons

$Vx_{OAAAspA} = Vx_{GluKGA}$ = 1 µmol/min/g; Rate of exchange from OAA to Asp in astroglia

$Vx_{OAAAspGA} = Vx_{GluKGGA}$ = 10 µmol/min/g; Rate of exchange from OAA to Asp in GABAergic neurons

$Vx_{OAAAspN} = Vx_{GluKGN}$ = 11.854 µmol/min/g; Rate of exchange from OAA to Asp in glutamatergic neurons

Values of Pool Concentrations:

Brain_Glucose1 = Vd*Km_in*((Vmax_in/CMRglc(ox)-1)*Blood_Glucose1-Km_in)/((Vmax_in/CMRglc(ox)+1)*Km_in+Blood_Glucose1) = 1.1622 µmol/g; Glucose concentration during [1-^{13}C]glucose infusion

Brain_Glucose2 = Vd*Km_in*((Vmax_in/CMRglc(ox)-1)*Blood_Glucose2-Km_in)/((Vmax_in/CMRglc(ox)+1)*Km_in+Blood_Glucose2) = 1.1508 µmol/g; Glucose concentration during [2-^{13}C]glucose infusion

P2 = P1 = 1.5 µmol/g; Tissue lactate concentration (Hawkins and Mans, 1983), P represents the pool of lactate and pyruvate, which are in rapid exchange (Mason et al., 1992)

AcCoAA2 = AcCoAA1 = 0.05 µmol/g; Acetyl-CoA in astroglia (Hawkins and Mans, 1983)

KGN2 = KGN1 = 0.1 µmol/g; KG in glutamatergic neurons, estimated from Hawkins and Mans (1983)

KGGA2 = KGGA1 = 0.01 µmol/g; KG in GABAergic neurons, estimated from Hawkins and Mans (1983)

KGA2 = KGA1 = 0.09 µmol/g; KG in astroglia, estimated from Hawkins and Mans (1983)

GluTotal2 = GluTotal1 = 13.56 µmol/g; Total Glu measured (from Glu H4 resonances)

GluN2 = GluN1 = GluTotal1-GluA1-GluGA1 = 11.933 µmol/g; Glu in glutamatergic neurons

GluGA2 = GluGA1= 0.02*GluTotal1 = 0.271 µmol/g; Glu in GABAergic neurons (small but indeterminate concentration; sensitivity tested and found to be small (Supplemental Information)

GluA2 = GluA1 = 0.1*GluTotal1 = 1.356 µmol/g; Glu in astroglia (Lebon et al., 2002, Tiwari et al., 2013, Lanz et al., 2014)

Gln2 = Gln1 = 5.85 µmol/g; Total Gln measured (from Gln H4 resonances)

GABA2 = GABA1 = 1.28 µmol/g; Total GABA pool measured (from GABA H3 resonances)

FumA2 = FumA1 = 0.01 µmol/g; Fum in astroglia, estimated from Hawkins and Mans (1983)

OAATotal2 = OAATotal1 = 0.2 µmol/g; Total tissue OAA (Hawkins and Mans, 1983)

OAAN2 = OAAN1 = 0.1 µmol/g; OAA in glutamatergic neurons, estimated from Hawkins and Mans (1983)

OAAGA2 = OAAGA1 = 0.05 µmol/g; OAA in GABAergic neurons, estimated from Hawkins and Mans (1983)

OAAA2 = OAAA1 = OAATotal1-OAAN1-OAAGA1 = 0.05 µmol/g; OAA in astroglia, estimated from Hawkins and Mans (1983)

AspTotal2 = AspTotal1 = 2.88 µmol/g; Total Asp pool measured (from Asp H3 resonances)

AspN2 = AspN1 = R_AspN_AspTot*AspTotal1 = 2.534 µmol/g; Asp in glutamatergic neurons (Ottersen and Storm-Mathisen, 1984, 1985, Zielinska et al., 2015)

AspGA2 = AspGA1= AspTotal1-AspA1-AspN1 = 0.058 µmol/g; Asp in GABAergic neurons (small but indeterminate concentration; sensitivity tested and found to be small (Supplemental Information)

AspA2 = AspA1 = R_AspA_AspTot*AspTotal1 = 0.288 µmol/g; Asp in astroglia (Ottersen and Storm-Mathisen, 1984, 1985, Zielinska et al., 2015)

Glc, glucose; P, pyruvate (represents the pool of lactate and pyruvate, which are in rapid exchange[1]); Glu, glutamate; Gln, glutamine; Asp, aspartate; OAA, oxaloacetate; KG, α-ketoglutarate; GABA: γ-aminobutyric acid (metabolites); Subscript 'N', 'GA' and 'A' stand for glutamatergic neurons, GABAergic neurons and astroglia (cellular compartments), respectively. '1' and '2' following metabolite pool abbreviation refers to the pool originating from [1-^{13}C]glucose and [2-^{13}C]glucose, respectively. Subscripted numbers represent the carbon position. Parameters listed in bold-faced type were determined by iterative fitting. References in the table are written in the format 'Author, year' in parenthesis, referring to reference number (Buschiazzo et al., 1970[2]; Hawkins and Mans, 1983[3]; Lanz et al., 2014[4]; Lebon et al., 2002[5]; Mason et al., 1992[1]; Ottersen and Storm-Mathisen, 1984[6], 1985[7]; Tiwari et al., 2013[8]; Zielinska et al., 2015[9]; Öz et al., 2004[10]).

Table S2. Mass of tissue samples (mg) from each region across all rats

	CX*	CB	HP	ST
Mean	275	214	106	46
SD	17	15	8	13
%SD	6	7	7	28
n-value	57	57	57	57

*250-300mg of the total collected cerebral cortex was extracted, hence not weight of total region.

Table S3. Regional metabolite concentrations

	Cerebral cortex		Cerebellum		Hippocampus		Striatum	
Glutamate	13.51 ± 0.95		11.64 ± 0.64		12.59 ± 0.90		13.73 ± 0.69	
Glutamine	5.82 ± 0.58		5.96 ± 0.51		5.50 ± 0.45		6.82 ± 0.46	
GABA	1.28 ± 0.12		1.18 ± 0.24		1.54 ± 0.14		2.01 ± 0.34	
Aspartate	2.87 ± 0.27		2.31 ± 0.21		2.31 ± 0.24		2.51 ± 0.21	
Alanine	0.64 ± 0.06		0.46 ± 0.11		0.75 ± 0.31		0.88 ± 0.10	
Lactate	2.90 ± 0.95		2.87 ± 1.68		3.02 ± 0.89		3.46 ± 0.70	
Glutamate	13.67	[12.67-14.12]	11.71	[11.31-12.05] *	12.81	[12-13.28] *,#	13.78	[13.21-14.15] #,§
Glutamine	5.61	[5.44-6.25]	5.95	[5.68-6.22]	5.48	[5.28-5.82] #	6.82	[6.47-7.09] *,#,§
GABA	1.27	[1.19-1.35]	1.13	[1.08-1.22]	1.55	[1.44-1.62] *,#	1.99	[1.76-2.19] *,#,§
Aspartate	2.81	[2.66-3.08]	2.31	[2.22-2.41] *	2.29	[2.15-2.48] *	2.48	[2.35-2.66] *,#,§
Alanine	0.63	[0.59-0.68]	0.45	[0.4-0.48] *	0.69	[0.64-0.75] #	0.88	[0.81-0.93] *,#,§
Lactate	2.77	[2.58-3.05]	2.58	[2.31-3.03]	2.81	[2.61-3.12]	3.40	[3.14-3.69] *,#,§

Results are presented as mean ± SD (upper panel) and median [IQR] (lower panel) in µmol/g wet tissue weight across all rats and time points. n_{CX}=45; n_{CB}=57; n_{HP}=36; n_{ST}=57 (n-values vary due to exclusion of samples not containing internal standard). Statistical comparisons of differences in metabolite levels across groups was conducted using the non-parametric Kruskal-Wallis test with Dunn's multiple comparison test due to some metabolites (10 of 24) having non-normal distributions. Asterisks (*) indicate metabolite levels significantly different ($p<0.05$) from that of cerebral cortex, hash tags ($^{\#}$) levels different from cerebellum, and section symbol (§) levels different from hippocampus.

Brain regional amino acid and metabolite concentrations in glucose-infused rats

Following euthanasia of the animals by FBMI the brain was removed and dissected into four regions, cerebral cortex (CX), cerebellum (CB), hippocampus (HP) and striatum (ST). Tissue mass variability (SD) was <7% for all regions except ST which varied by 28% (**Table S2**). Total metabolite concentrations obtained from non-edited ^{1}H-[^{13}C]NMR spectra showed multiple, significant differences between brain regions (**Table S3)**. In brief, Glu concentration was highest in ST and CX, intermediate in HP, and lowest in CB. Likewise, Gln and Asp concentrations were lowest in CB and HP and highest in ST and CX. The concentrations of GABA, alanine and lactate were lowest in CB and increased in the order CX<HP<ST.

Comparison of general measures with previously reported values

The measured blood plasma glucose concentrations and enrichments (**Figure S1**) are in line with values reported previously[11, 12]. Likewise, plasma glutamine concentrations agree with earlier rodent data[13, 14]. In particular, Dadmarz et al.[14] reports an increased glutamine plasma level in fasted compared to fed rats (0.84±0.14 mM versus 0.50±0.06 mM), consistent with the levels we observed for the fasted animals in our study (0.79-0.80 mM). The average brain tissue concentrations measured for glutamate, glutamine, GABA, aspartate, alanine and lactate (**Table S3**) in the current study are in agreement with earlier studies[12, 15], as well as the differences in relative glutamate and GABA concentrations between brain regions[15].

Table S4. Additional metabolic fluxes (µmol/g/min) across brain regions derived from the three-compartment model

		Cerebral cortex			Cerebellum			Hippocampus			Striatum		
Iterated fluxes	$PercVtca_{GANet}$	84.32 ± 7.35	81.97 [76.81 - 86.66]	Yes	44.88 ± 9.52	43.58 [37.09 - 49.75]	Yes	88.83 ± 7.67	88.90 [83.08 - 93.94]	No	88.79 ± 9.84	88.74 [80.53 - 96.91]	No
	$R\_Vdil_{Gln}\_Vgln$	0.270 ± 0.02	0.281 [0.266 - 0.295]	Yes	0.470 ± 0.035	0.467 [0.446 - 0.491]	No	0.268 ± 0.03	0.278 [0.26 - 0.295]	No	0.303 ± 0.040	0.312 [0.285 - 0.340]	No
	$Vcyc_{GABAGln}$	0.109 ± 0.015	0.105 [0.095 - 0.115]	Yes	0.075 ± 0.011	0.075 [0.068 - 0.083]	No	0.079 ± 0.016	0.079 [0.068 - 0.090]	Yes	0.083 ± 0.021	0.084 [0.069 - 0.099]	No
	$Vcyc_{GluGln}$	0.700 ± 0.073	0.696 [0.648 - 0.743]	No	0.444 ± 0.051	0.447 [0.417 - 0.482]	No	0.716 ± 0.084	0.708 [0.659 - 0.764]	No	0.811 ± 0.100	0.800 [0.731 - 0.867]	No
	$Vdil_{A\_In}$	0.090 ± 0.022	0.089 [0.077 - 0.105]	No	0.050 ± 0.017	0.049 [0.039 - 0.061]	Yes	0.115 ± 0.025	0.122 [0.105 - 0.138]	No	0.107 ± 0.034	0.114 [0.093 - 0.138]	No
	$Vdil_{GA}$	0.090 ± 0.010	0.090 [0.084 - 0.097]	Yes	0.066 ± 0.007	0.066 [0.061 - 0.071]	Yes	0.096 ± 0.014	0.096 [0.088 - 0.106]	No	0.096 ± 0.018	0.097 [0.085 - 0.110]	No
	$Vdil_{N}$	0.127 ± 0.036	0.122 [0.095 - 0.144]	Yes	0.061 ± 0.027	0.059 [0.043 - 0.078]	No	0.086 ± 0.033	0.078 [0.056 - 0.100]	No	0.023 ± 0.031	0.000 [0.000 - 0.034]	No
	$Vpdh_{A}$	0.126 ± 0.028	0.132 [0.117 - 0.150]	No	0.198 ± 0.036	0.196 [0.171 - 0.217]	Yes	0.078 ± 0.029	0.091 [0.074 - 0.109]	No	0.118 ± 0.056	0.138 [0.108 - 0.176]	No
	$Vpdh_{GA}$	0.229 ± 0.016	0.224 [0.214 - 0.236]	No	0.187 ± 0.011	0.187 [0.180 - 0.194]	No	0.201 ± 0.020	0.199 [0.187 - 0.215]	No	0.180 ± 0.020	0.178 [0.165 - 0.192]	No
	$Vtca_{ANet}$	0.001 ± 0.024	0.000 [0.000 - 0.020]	No	0.086 ± 0.036	0.082 [0.056 - 0.106]	No	0.000 ± 0.032	0.000 [0.000 - 0.034]	No	0.017 ± 0.060	0.024 [0.000 - 0.081]	No
	$Vtca_{N}$	1.268 ± 0.038	1.252 [1.227 - 1.276]	Yes	0.962 ± 0.037	0.968 [0.943 - 0.994]	Yes	0.883 ± 0.036	0.858 [0.833 - 0.881]	No	1.164 ± 0.060	1.130 [1.096 - 1.170]	Yes
	Vx_{GluKGN}	11.85 ± 6.864	10.72 [8.723 - 14.37]	No	5.10 ± 1.83	5.19 [4.46 - 6.10]	No	10.80 ± 27.61	10.30 [7.23 - 16.02]	No	6.09 ± 2.31	5.33 [4.47 - 6.45]	No
Calculated fluxes	$CMRglc(ox)$	0.802 ± 0.012	0.800 [0.791 - 0.808]	No	0.686 ± 0.011	0.688 [0.682 - 0.695]	No	0.595 ± 0.013	0.594 [0.584 - 0.603]	No	0.782 ± 0.021	0.784 [0.769 - 0.798]	Yes
	$Vdil_{Gln}$	0.247 ± 0.016	0.254 [0.243 - 0.266]	No	0.285 ± 0.017	0.286 [0.276 - 0.298]	Yes	0.243 ± 0.018	0.251 [0.239 - 0.264]	Yes	0.308 ± 0.027	0.316 [0.295 - 0.333]	No
	Vefflux	0.353 ± 0.019	0.361 [0.349 - 0.375]	No	0.372 ± 0.019	0.374 [0.361 - 0.387]	Yes	0.357 ± 0.020	0.367 [0.354 - 0.381]	Yes	0.433 ± 0.030	0.445 [0.425 - 0.466]	Yes
	Vgad	0.159 ± 0.014	0.161 [0.152 - 0.171]	No	0.214 ± 0.021	0.217 [0.204 - 0.232]	No	0.112 ± 0.013	0.112 [0.104 - 0.121]	No	0.114 ± 0.017	0.115 [0.104 - 0.125]	No
	Vgln	0.915 ± 0.075	0.907 [0.861 - 0.956]	No	0.606 ± 0.052	0.611 [0.578 - 0.646]	No	0.909 ± 0.084	0.905 [0.851 - 0.961]	No	1.019 ± 0.100	1.013 [0.945 - 1.082]	No
	Vpc	0.106 ± 0.005	0.108 [0.104 - 0.110]	Yes	0.087 ± 0.004	0.087 [0.084 - 0.090]	Yes	0.114 ± 0.005	0.116 [0.113 - 0.119]	No	0.125 ± 0.009	0.130 [0.124 - 0.137]	No
	$Vpdh_{N}$	1.142 ± 0.033	1.133 [1.111 - 1.153]	No	0.901 ± 0.032	0.907 [0.887 - 0.928]	Yes	0.797 ± 0.036	0.780 [0.755 - 0.804]	Yes	1.141 ± 0.055	1.114 [1.078 - 1.147]	No
	Vsc	0.080 ± 0.010	0.082 [0.077 - 0.089]	No	0.092 ± 0.013	0.091 [0.082 - 0.099]	Yes	0.071 ± 0.012	0.077 [0.071 - 0.085]	No	0.083 ± 0.024	0.091 [0.079 - 0.109]	No
	$Vtca_{A}$	0.217 ± 0.027	0.221 [0.209 - 0.240]	No	0.248 ± 0.036	0.247 [0.221 - 0.268]	Yes	0.193 ± 0.034	0.208 [0.192 - 0.230]	No	0.226 ± 0.066	0.246 [0.214 - 0.294]	No
	$Vtca_{ANetprime}$	0.190 ± 0.036	0.196 [0.179 - 0.221]	No	0.253 ± 0.046	0.251 [0.217 - 0.279]	Yes	0.150 ± 0.044	0.169 [0.149 - 0.199]	No	0.184 ± 0.085	0.210 [0.165 - 0.271]	No
	$Vtca_{GA}$	0.320 ± 0.022	0.314 [0.301 - 0.330]	No	0.253 ± 0.013	0.253 [0.244 - 0.261]	No	0.297 ± 0.030	0.296 [0.277 - 0.316]	No	0.276 ± 0.033	0.275 [0.254 - 0.297]	No
	$Vtca_{Tot}$	1.805 ± 0.035	1.793 [1.769 - 1.816]	Yes	1.464 ± 0.031	1.465 [1.445 - 1.486]	No	1.372 ± 0.038	1.369 [1.346 - 1.396]	No	1.665 ± 0.054	1.670 [1.634 - 1.704]	No
	Vx_{KGGluA}	1.215 ± 0.015	1.213 [1.202 - 1.223]	Yes	1.162 ± 0.011	1.162 [1.156 - 1.170]	No	1.193 ± 0.016	1.195 [1.185 - 1.207]	No	1.208 ± 0.022	1.214 [1.199 - 1.231]	Yes

Best-fit metabolic fluxes ± MC SD and MC median[IQR] are given for $PercVtca_{GANet}$: The amount of the GABAergic TCA cycle (as percentage) that continues beyond alpha-ketoglutarate (KG) through oxaloacetate; $R\_VdilGln\_Vgln$: Ratio between $Vdil_{Gln}$ and Vgln; CMRglc(ox): Glucose consumption rate; $Vcyc_{GluGln}$: rate of glutamate-glutamine cycling; $Vcyc_{GABAGln}$: rate of GABA-glutamine cycling; Vdil: Rate of unspecific dilution in either of the three compartments, i.e. the glutamatergic neuron ($Vdil_{N}$), the GABAergic neuron ($Vdil_{GA}$) or the astroglia ($Vdil_{A\_In}$); $Vdil_{Gln}$: Rate introducing unlabeled glutamine from the blood to the brain; Vefflux: Rate of loss of carbon from the astroglial TCA cycle via efflux of Gln from the brain, partly balanced by entry of glutamine from the blood, also at the rate $Vdil_{Gln}$; Vgad: rate of GABA synthesis via glutamate decarboxylase (GAD); Vgln: rate of glutamine synthesis via glutamine synthetase; Vpc: rate of pyruvate carboxylase; Vpdh: Rate of pyruvate dehydrogenase (PDH) activity in the glutamatergic neuron ($Vpdh_{N}$), the GABAergic neuron ($Vpdh_{GA}$) and the astroglia ($Vpdh_{A}$); Vsc: Rate of scrambling; Vtca: Rate of TCA cycle activity in the glutamatergic neuron ($Vtca_{N}$), the GABAergic neuron ($Vtca_{GA}$) and the astroglia ($Vtca_{A}$: flow from citric acid through KG; $Vtca_{ANet}$: flow from KG to succinate; $Vtca_{ANetprime}$: flow from succinate to OAA); $Vtca_{Tot}$: ($=Vtca_{N}+Vtca_{A}+Vtca_{GA}$) rate of total TCA cycle; Vx_{KGGlu}: Exchange rate between alpha-ketoglutarate (KG) and glutamate (Glu) in astroglia (Vx_{KGGluA}) and glutamatergic neurons (Vx_{KGGluN}). Yes/no: Indicates if the rate distribution passed Shapiro-Wilk test for normality. MC SD, standard deviation calculaed from Monte-Carlo simulations; IQR, 25% to 75% Interquartile Range.

Table S5. Metabolic fluxes (µmol/g/min) across brain regions derived from the two-compartment model

		Cerebral cortex			Cerebellum			Hippocampus			Striatum		
Iterated fluxes	R_Vdil$_{Gln}$_Vgln	0.292 ± 0.026	0.292 [0.278-0.312]	No	0.537 ± 0.044	0.541 [0.513-0.569]	No	0.286 ± 0.027	0.291 [0.273-0.310]	No	0.336 ± 0.048	0.338 [0.310-0.374]	No
	Vcyc$_{GluGln}$	0.815 ± 0.082	0.808 [0.757-0.858]	No	0.449 ± 0.049	0.447 [0.413-0.483]	No	0.839 ± 0.080	0.813 [0.756-0.867]	Yes	0.862 ± 0.107	0.852 [0.767-0.920]	No
	Vdil$_{A_in}$	0.075 ± 0.025	0.079 [0.064-0.097]	No	0.033 ± 0.024	0.034 [0.017-0.050]	No	0.077 ± 0.023	0.080 [0.066-0.094]	No	0.078 ± 0.037	0.080 [0.055-0.105]	No
	Vdil$_{N}$	0.141 ± 0.039	0.136 [0.113-0.161]	No	0.078 ± 0.029	0.075 [0.053-0.092]	No	0.106 ± 0.036	0.111 [0.088-0.134]	Yes	0.047 ± 0.043	0.046 [0.016-0.078]	No
	Vpdh$_{A}$	0.103 ± 0.041	0.114 [0.087-0.139]	No	0.268 ± 0.044	0.270 [0.250-0.303]	No	0.030 ± 0.029	0.043 [0.027-0.065]	No	0.108 ± 0.066	0.123 [0.080-0.180]	No
	Vtca$_{ANet}$	0.070 ± 0.037	0.083 [0.061-0.106]	No	0.215 ± 0.036	0.220 [0.202-0.247]	No	0.000 ± 0.029	0.006 [0.000-0.032]	No	0.066 ± 0.065	0.079 [0.036-0.122]	No
	Vtca$_{N}$	1.406 ± 0.044	1.396 [1.368-1.425]	Yes	1.002 ± 0.041	0.995 [0.967-1.020]	Yes	1.041 ± 0.038	1.030 [1.003-1.056]	Yes	1.259 ± 0.066	1.252 [1.208-1.297]	No
	Vx$_{GluKGN}$	18.91 ± 8.92	19.16 [14.17-25.19]	No	6.64 ± 3.50	6.54 [5.55-7.77]	No	9.99 ± 10.20	10.17 [7.71-13.76]	No	7.97 ± 5.16	7.856 [6.11-10.37]	No
Calculated fluxes	CMRglc(ox)	0.738 ± 0.012	0.741 [0.733-0.749]	No	0.639 ± 0.012	0.641 [0.633-0.649]	No	0.536 ± 0.011	0.537 [0.529-0.545]	Yes	0.720 ± 0.021	0.727 [0.711-0.740]	Yes
	Vdil$_{Gln}$	0.270 ± 0.018	0.271 [0.257-0.283]	No	0.287 ± 0.018	0.289 [0.276-0.300]	No	0.270 ± 0.019	0.268 [0.255-0.281]	Yes	0.330 ± 0.030	0.330 [0.307-0.349]	Yes
	Vefflux	0.378 ± 0.020	0.382 [0.366-0.394]	No	0.374 ± 0.020	0.376 [0.363-0.390]	No	0.377 ± 0.021	0.377 [0.362-0.390]	Yes	0.450 ± 0.033	0.452 [0.430-0.475]	Yes
	Vgln	0.923 ± 0.080	0.915 [0.867-0.967]	No	0.535 ± 0.049	0.535 [0.499-0.573]	No	0.946 ± 0.081	0.922 [0.861-0.977]	Yes	0.982 ± 0.106	0.970 [0.888-1.042]	No
	Vpc	0.108 ± 0.005	0.110 [0.107-0.113]	Yes	0.086 ± 0.005	0.087 [0.084-0.091]	Yes	0.107 ± 0.004	0.108 [0.105-0.111]	Yes	0.121 ± 0.009	0.124 [0.117-0.130]	Yes
	Vpdh$_{N}$	1.265 ± 0.041	1.257 [1.234-1.286]	Yes	0.924 ± 0.037	0.920 [0.893-0.946]	Yes	0.935 ± 0.036	0.922 [0.896-0.943]	No	1.212 ± 0.059	1.201 [1.165-1.241]	No
	Vsc	0.066 ± 0.015	0.071 [0.062-0.080]	No	0.111 ± 0.014	0.114 [0.106-0.124]	No	0.040 ± 0.011	0.042 [0.04-0.0520]	No	0.069 ± 0.026	0.074 [0.059-0.094]	No
	Vtca$_{A}$	0.179 ± 0.040	0.191 [0.169-0.216]	No	0.301 ± 0.039	0.307 [0.287-0.336]	No	0.107 ± 0.030	0.114 [0.108-0.141]	No	0.186 ± 0.069	0.201 [0.160-0.254]	No
	Vtca$_{ANetprime}$	0.137 ± 0.052	0.153 [0.123-0.186]	No	0.326 ± 0.050	0.334 [0.309-0.371]	No	0.040 ± 0.040	0.048 [0.040-0.085]	No	0.135 ± 0.090	0.153 [0.096-0.214]	No
	Vtca$_{Tot}$	1.585 ± 0.036	1.588 [1.564-1.613]	Yes	1.303 ± 0.030	1.305 [1.285-1.325]	Yes	1.148 ± 0.032	1.158 [1.136-1.183]	Yes	1.445 ± 0.051	1.455 [1.428-1.498]	Yes
	Vx$_{KGGluA}$	1.108 ± 0.005	1.110 [1.106-1.113]	Yes	1.086 ± 0.005	1.087 [1.084-1.091]	Yes	1.107 ± 0.004	1.108 [1.105-1.111]	Yes	1.121 ± 0.009	1.123 [1.117-1.130]	Yes

Best-fit metabolic fluxes ± MC SD and MC median[IQR] are given for R_VdilGln_Vgln: Ratio between Vdil$_{Gln}$ and Vgln; CMRglc(ox): Glucose consumption rate; Vcyc$_{GluGln}$: rate of glutamate-glutamine cycling; Vdil: Rate of unspecific dilution in either of the two compartments, i.e. the neuronal (Vdil$_{N}$) or the astroglia compartment (Vdil$_{A_in}$); Vdil$_{Gln}$: Rate introducing unlabeled glutamine from the blood to the brain; Vefflux: Rate of loss of carbon from the astroglial TCA cycle via efflux of Gln from the brain, partly balanced by entry of glutamine from the blood, also at the rate Vdil$_{Gln}$; Vgln: rate of glutamine synthesis via glutamine synthetase; Vpc: rate of pyruvate carboxylase; Vpdh: Rate of pyruvate dehydrogenase (PDH) activity in the neuronal (Vpdh$_{N}$) and the astroglia (Vpdh$_{A}$); Vsc: Rate of scrambling; Vtca: Rate of TCA cycle activity in the neuronal (Vtca$_{N}$) and the astroglia compartment (Vtca$_{A}$: flow from citric acid through KG; Vtca$_{ANet}$: flow from KG to succinate; Vtca$_{ANetprime}$: flow from succinate to OAA); Vtca$_{Tot}$: (=Vtca$_{N}$+Vtca$_{A}$) rate of total TCA cycle; Vx$_{KGGlu}$: Exchange rate between alpha-ketoglutarate (KG) and glutamate (Glu) in astroglia (Vx$_{KGGluA}$) and neurons (Vx$_{KGGluN}$). Yes/no: Indicates if the rate distribution passed the Shapiro-Wilk test for normality. MC SD, standard deviation calculaed from Monte-Carlo simulations; IQR, 25% to 75% Interquartile Range.

Supplementary information for Rates of pyruvate carboxylase, glutamate and GABA neurotransmitter cycling, and glucose oxidation in multiple brain regions of the awake rat using a combination of [2-^{13}C]/[1-^{13}C]glucose infusion and ^{1}H-[^{13}C]NMR *ex vivo,* by LM McNair *et al.* 2021, JCBFM

Supplementary figures

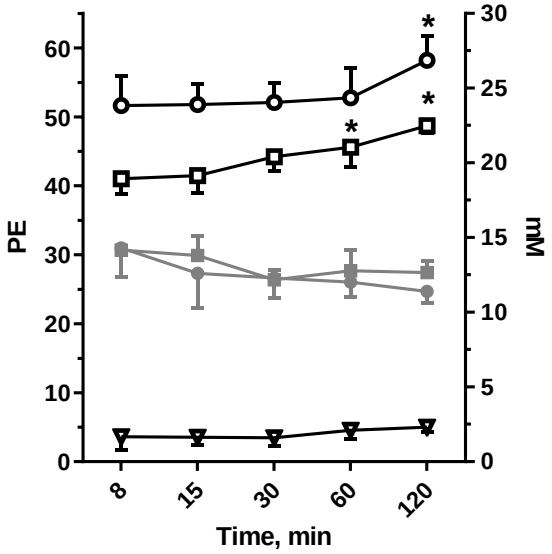

Figure S1. Blood plasma glucose concentrations (mM; grey symbols, right y-axis) and C1 and C2 percentage ^{13}C-enrichment (PE; black hollow symbols, left y-axis) following 8-120 min infusions with [1-^{13}C]glucose (circles) or [2-^{13}C]glucose (squares), respectively, and PE at glucose-C1 following [2-^{13}C]glucose infusions (triangles) normalized to glucose-C2 PE. All plasma data passed the Shapiro-Wilk test for normality. Results are presented as mean and SD of data obtained from 5-7 rats per time point for each ^{13}C-substrate. Blood plasma glucose concentrations from rats infused with [1-^{13}C]glucose and [2-^{13}C]glucose, respectively, were not significantly different at any time point (multiple unpaired Student's t-tests, corrected for multiple comparisons using the Holm- Šídák method) with an overall average of 12.7±1.8 mM (n=27) and 13.2±1.2 mM (n=30), respectively. The PE of glucose-C1 and -C2 were stable except for a significant increase at 120 min (C1) and at 60min and 120 min (C2) (*: $p<0.05$, one-way ANOVA followed by Dunnett's multiple comparisons test). The PE of glucose-C1 obtained by [1-^{13}C]glucose infusions was significantly higher compared to PE at glucose-C2 obtained by infusions with [2-^{13}C]glucose at all five time points (multiple unpaired Student's t-test, corrected for multiple comparisons using the Holm- Šídák method). The difference in PE's of the two substrates could not be explained by differences in other measures such as fasting time (18±2 hours and 17±2 hours; $p=0.6$, unpaired Student's t-test), time of year the experiments were conducted (fall/spring=21/6 and 15/15; Chi square with Yates correction, $p=0.06$) or spectral integration approaches for glucose-C1 and -C2, α and β. Because we did not independently verify the ^{13}C enrichments of the [1-^{13}C]- and [2-^{13}C] glucose supplied by the manufacturer, we cannot exclude the possibility that they differed.

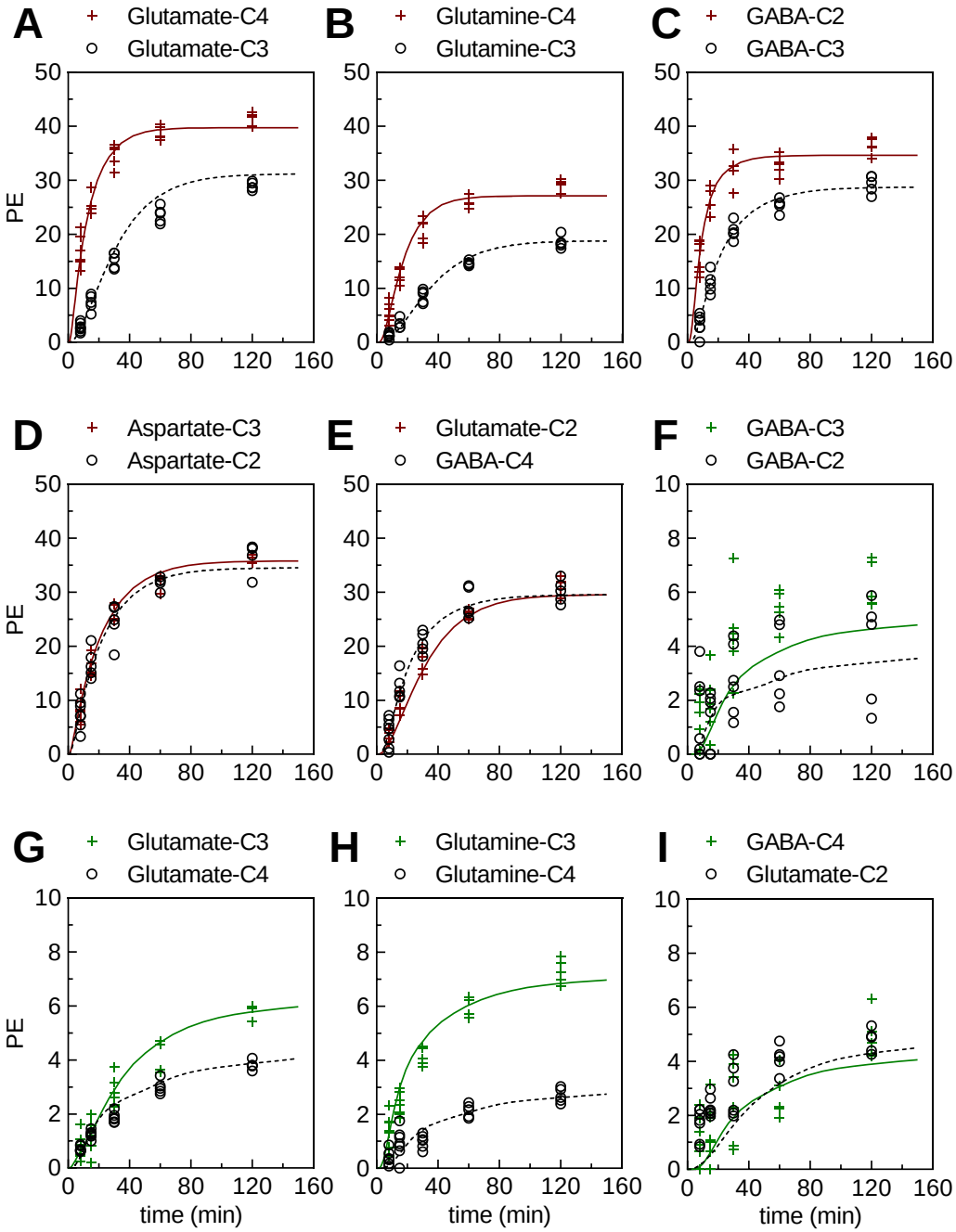

Figure S2. Fits of the metabolic model (full green or dotted black lines) to experimental data from cerebellum (green plus and black circle symbols, respectively). The time courses for percentage ^{13}C-enrichment (PE) of (**A-E**) glutamate-C4,C3,C2, glutamine-C4,C3, GABA-C2,C3,C4, and aspartate-C2,C3 from [1-^{13}C]glucose or (**F-I**) glutamate-C4,C3,C2, glutamine-C4,C3, and GABA-C2,C3,C4 from [2-^{13}C]glucose infused rats obtained with ^{1}H-[^{13}C]NMR. A majority (83 of the 90) of the time course data sets from cerebellum (n=5-7 for each time point) passed the Shapiro-Wilk test for normality.

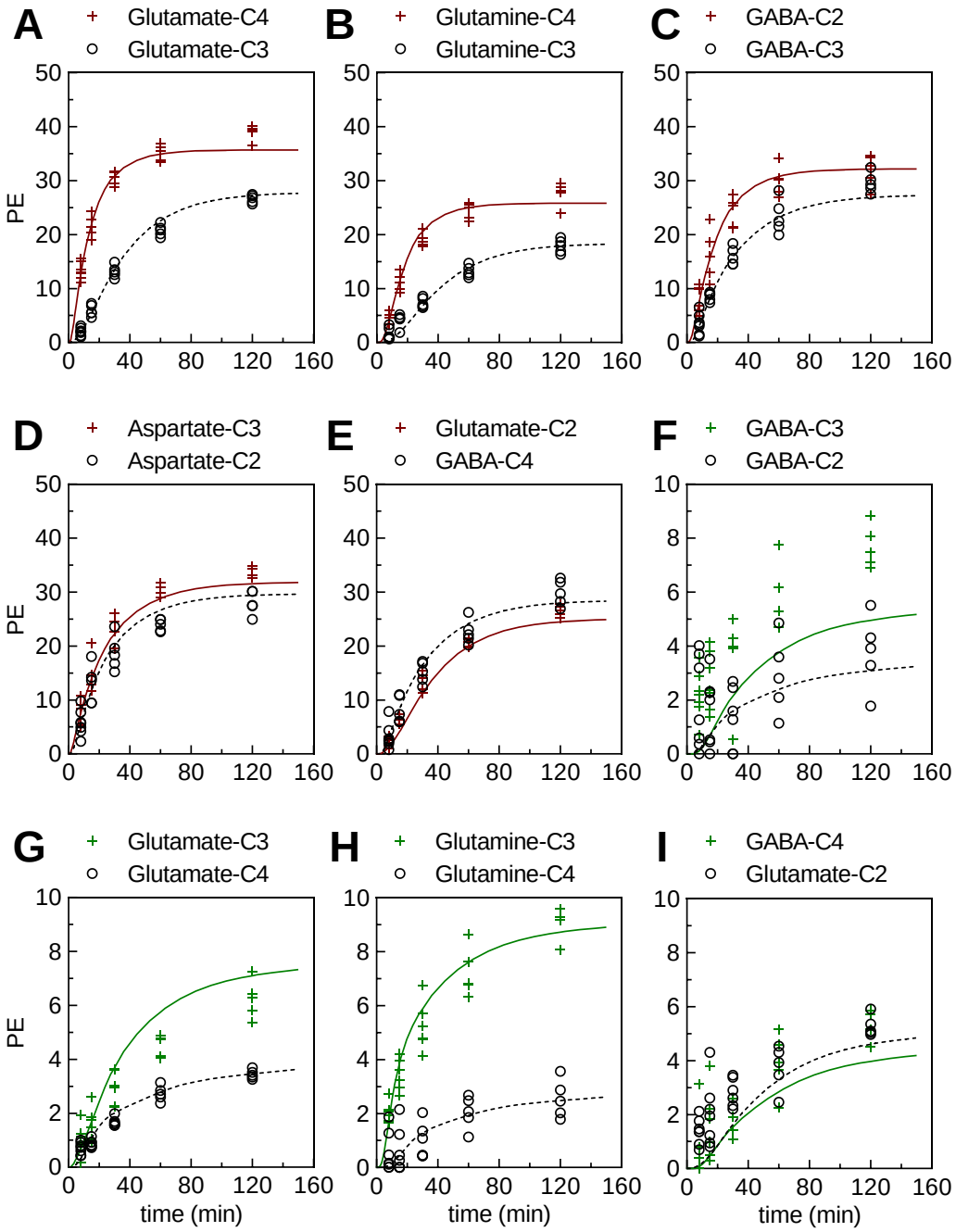

Figure S3. Fits of the metabolic model (full green or dotted black lines) to experimental data from hippocampus (green plus and black circle symbols, respectively). The time courses for percentage ^{13}C-enrichment (PE) of (**A-E**) glutamate-C4,C3,C2, glutamine-C4,C3, GABA-C2,C3,C4, and aspartate-C2,C3 from [1-^{13}C]glucose or (**F-I**) glutamate-C4,C3,C2, glutamine-C4,C3, and GABA-C2,C3,C4 from [2-^{13}C]glucose infused rats obtained with ^{1}H-[^{13}C]NMR. A majority (83 of the 90) of the time course data sets from hippocampus (n=5-7 for each time point) passed the Shapiro-Wilk test for normality.

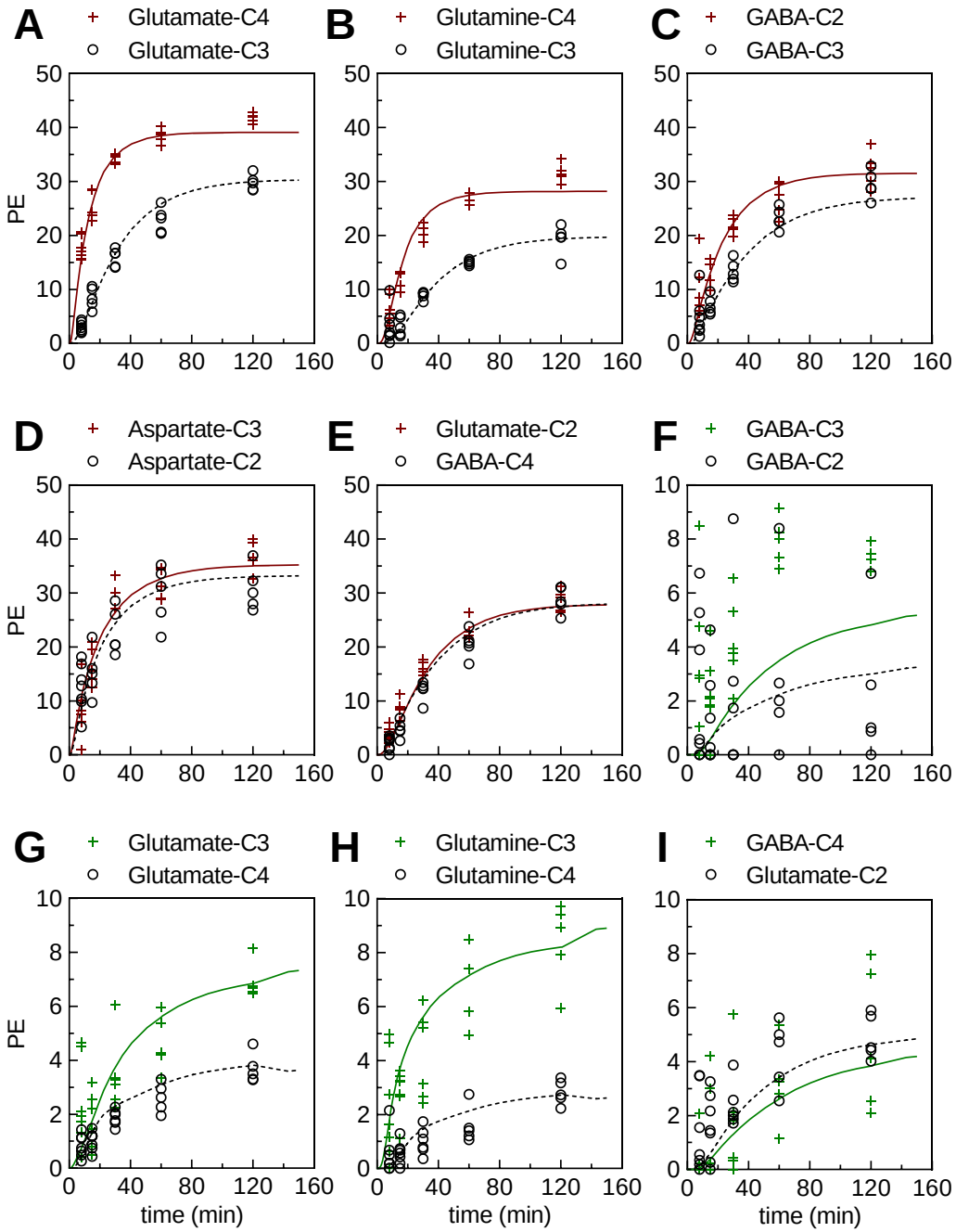

Figure S4. Fits of the metabolic model (full green or dotted black lines) to experimental data from striatum (green plus and black circle symbols, respectively). The time courses for percentage ^{13}C-enrichment (PE) of (**A-E**) glutamate-C4,C3,C2, glutamine-C4,C3, GABA-C2,C3,C4, and aspartate-C2,C3 from [1-^{13}C]glucose or (**F-I**) glutamate-C4,C3,C2, glutamine-C4,C3, and GABA-C2,C3,C4 from [2-^{13}C]glucose infused rats obtained with ^{1}H-[^{13}C]NMR. A majority (80 of the 90) of the time course data sets from striatum (n=5-7 for each time point) passed the Shapiro-Wilk test for normality.

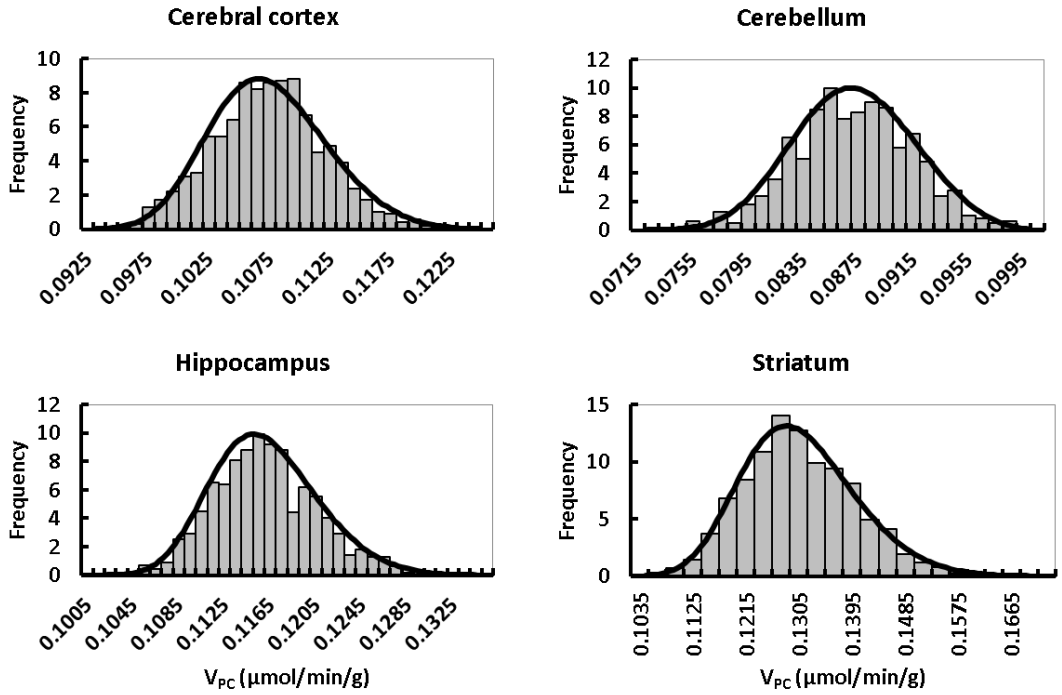

Figure S5. Frequency distributions for the rate of pyruvate carboxylase (Vpc) obtained from 1000 Monte Carlo simulations of the three-compartment model best-fit solutions to the time course data from cerebral cortex, cerebellum, hippocampus and striatum. The distribution approximated a normal function for cerebellum (Shipiro-Wilk test, W=0.998, P=0.449) but not for the other regions (cortex, P=0.021; hippocampus, P=0.0002; striatum, P<0.0001) which tended to skew slightly to higher values.

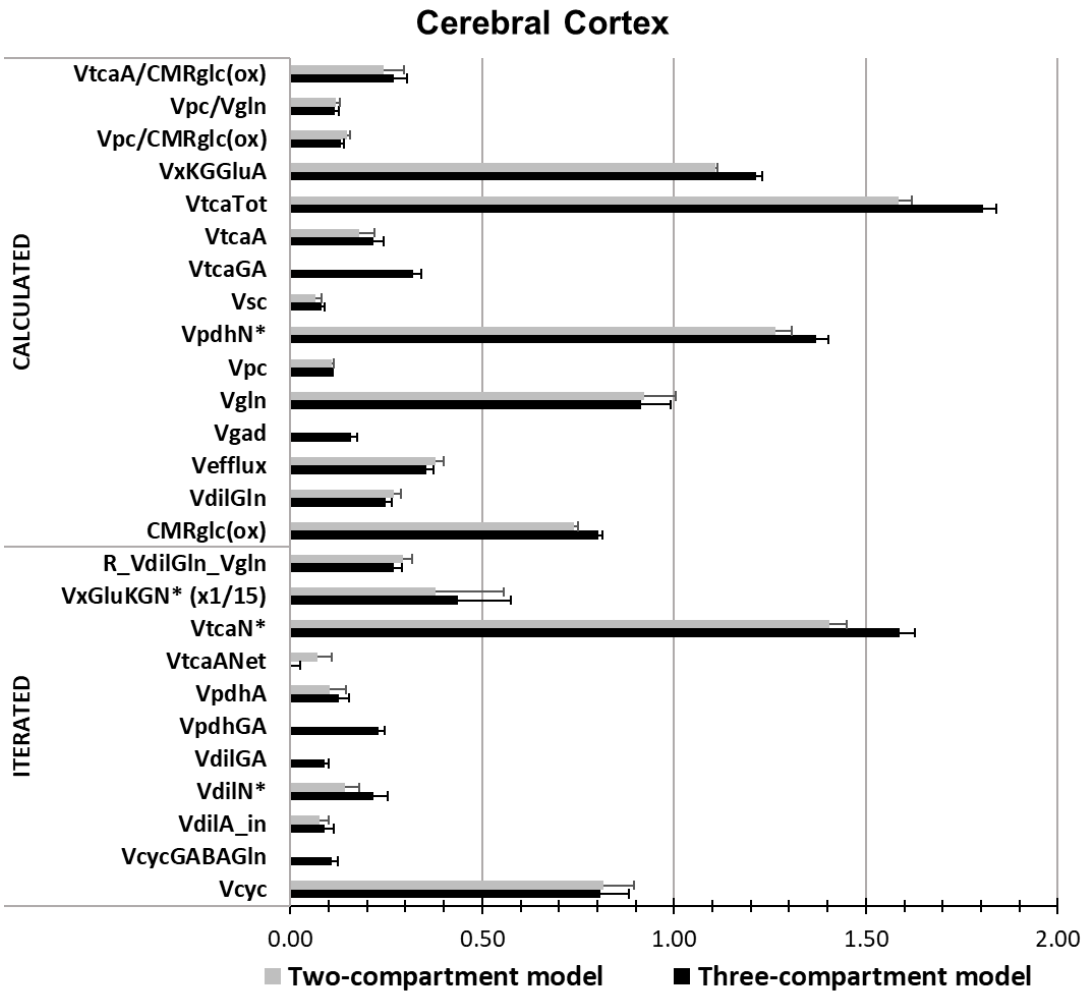

Figure S6. Comparison of the best-fit metabolic fluxes for cerebral cortex determined by the three-compartment model (black bars) verses a two-compartment (gray bars) model. R_VdilGln_Vgln: Ratio between VdilGln and Vgln; CMRglc(ox): Glucose consumption rate; Vcyc: rate of glutamate/GABA-glutamine cycling; VcycGABAGln; rate of GABA-glutamine cycling; Vdil: Rate of unspecific dilution in either of two compartments, i.e. the neuronal (VdilN*), the GABAergic neuronal (VdilGA) or the astroglia (VdilA_in); VdilGln: Rate introducing unlabeled glutamine from the blood to the brain; Vgad: rate of GABA synthesis via glutamate decarboxylase (GAD); Vefflux: Rate of loss of carbon from the astroglial TCA cycle via efflux of Gln from the brain, partly balanced by entry of glutamine from the blood, also at the rate VdilGln; Vgln: rate of glutamine synthesis via glutamine synthetase; Vpc: rate of pyruvate carboxylase; Vpdh: Rate of pyruvate dehydrogenase (PDH) activity in the neuronal compartment (VpdhN*), the GABAergic neruonal compartment (VpdhGA) and the astroglia (VpdhA); Vsc: Rate of scrambling; Vtca: Rate of TCA cycle activity in the neuronal compartment (VtcaN*), the GABAergic neuronal compartment (VtcaGA) and the astroglia (VtcaA: flow from citric acid through KG; VtcaANet: flow from KG through succinate); VtcaTot: (=VtcaN*+VtcaA) rate of total TCA cycle; VxKGGlu: Exchange rate between alpha-ketoglutarate (KG) and glutamate (Glu) in astroglia (VxKGGluA) and neurons (VxKGGluN*). N* designates the neuronal compartment and for the case of the three-compartment model, reflects the sum of the glutamatergic and GABAergic neuronal rates, e.g. VtcaN* = VtcaN + VtcaGA. MC SDs for the N* best estimates were determined as the variance for data set resulting from summing each of the 1000 MC (Monte Carlo analysis) iterations. Ratios between rates calculated post hoc are listed as V_i/V_j, e.g. Vpc/Vgln.

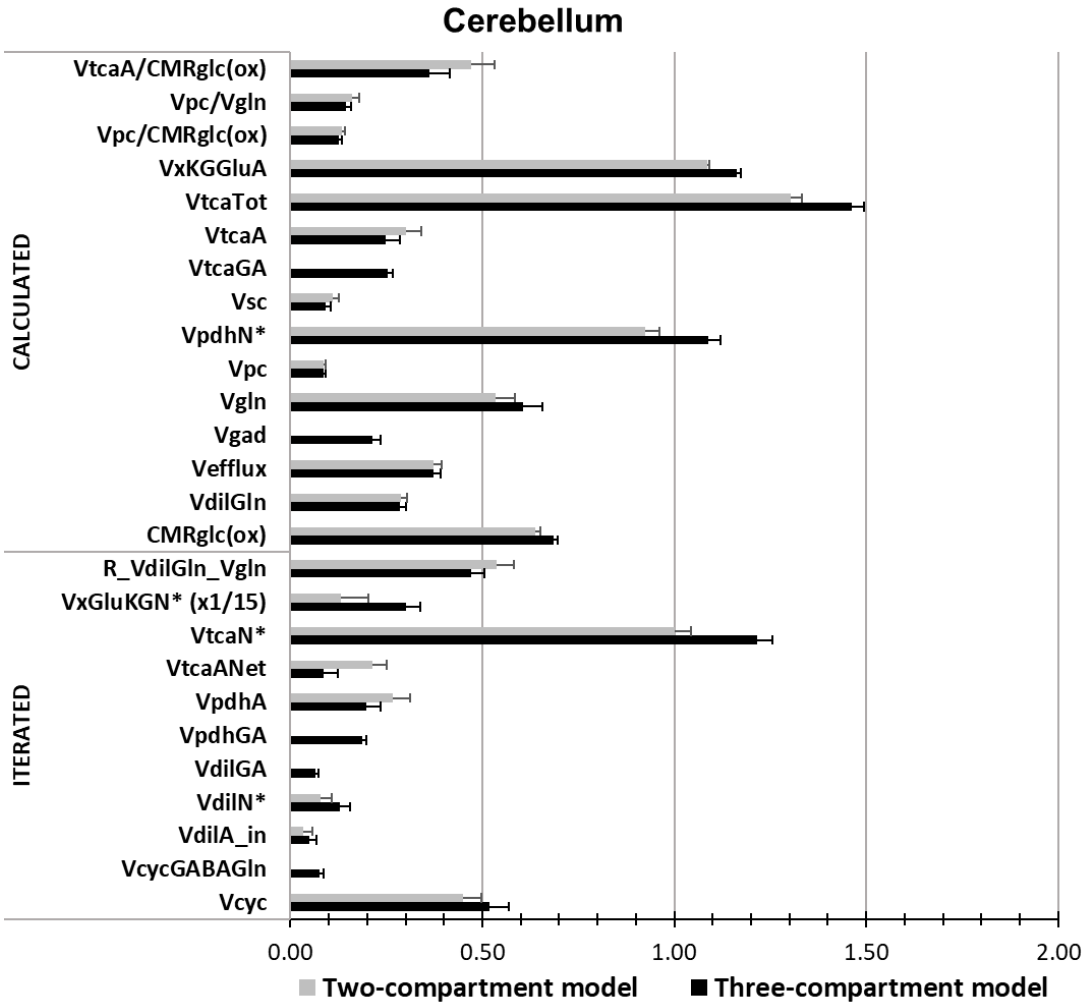

Figure S7. Comparison of the best-fit metabolic fluxes for cerebellum determined by the three-compartment model (black bars) verses a two-compartment (gray bars) model. See legend **Figure S6** for definitions and further details.

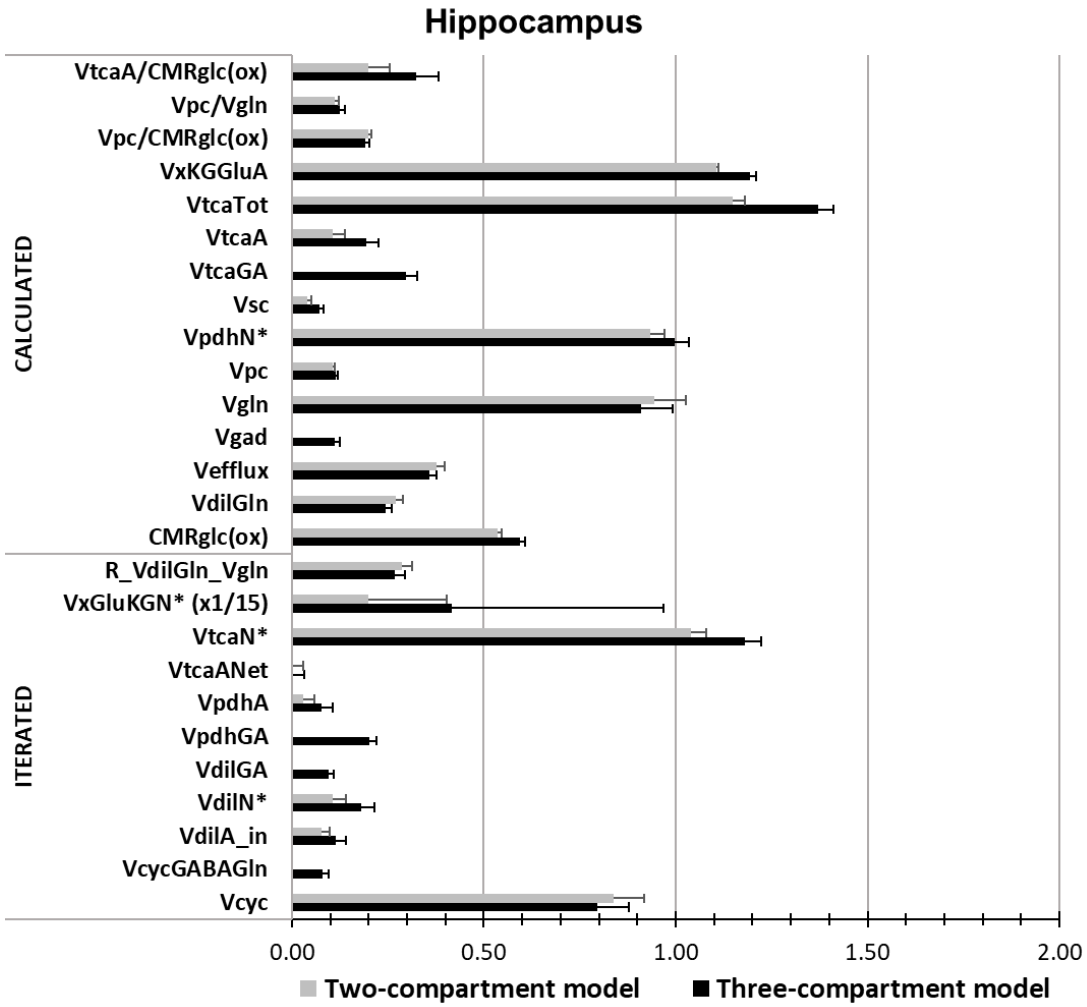

Figure S8. Comparison of the best-fit metabolic fluxes for hippocampus determined by the three-compartment model (black bars) verses a two-compartment (gray bars) model. See legend **Figure S6** for definitions and further details.

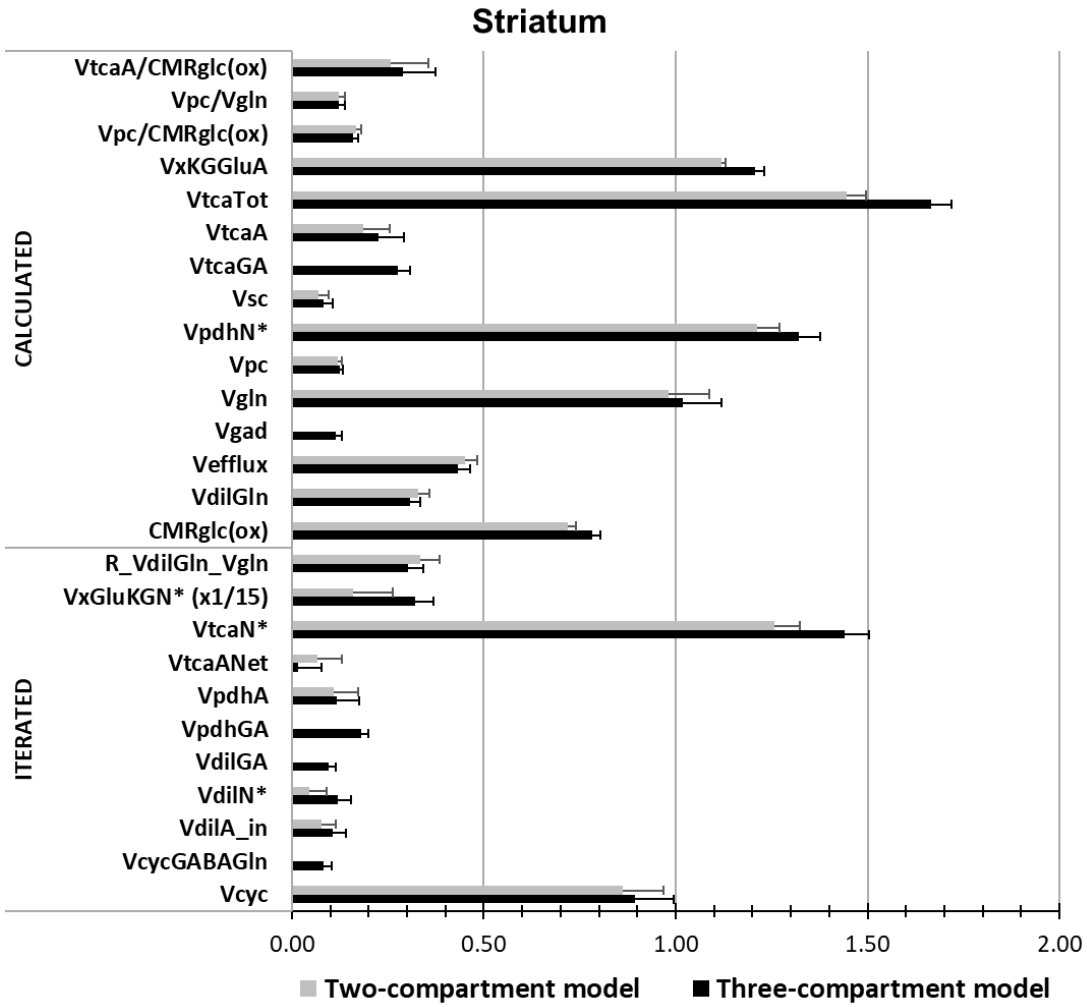

Figure S9. Comparison of the best-fit metabolic fluxes for striatum determined by the three-compartment model (black bars) verses a two-compartment (gray bars) model. See legend **Figure S6** for definitions and further details.

Supplementary results – Sensitivity analysis

The local sensitivity of the metabolic model to certain parameters, which are either unknown or poorly determined and constrained as fixed values in the model, were tested one at a time using cerebral cortex data. Best fits were obtained for the values of Vpc, as well as $Vcyc_{GluGln}$, $Vcyc_{GABAGln}$, $Vtca_{Tot}$, Vgad and Vgln by successively varying the test (fixed) parameter for a range above and below their nominal (assumed) values. This analysis indicates the magnitude and trajectory of deviations expected in the determined fluxes should the true value of the tested parameter differ from the nominal value.

The tests revealed that, whereas the value of Vpc was relatively insensitive to the size of the astroglial aspartate and glutamate pool fractions, and the astroglial α-ketoglutarate/glutamate exchange rate, it was particularly sensitive to the degree of label scrambling at the fumarate step, where Vpc varied -15 to +35% from the nominal value for $Vsc/Vtca_A$ ratios ranging from 0 to 3. Likewise, $Vcyc_{GABAGln}$, $Vcyc_{GluGln}$, and Vgln, but not $Vtca_{Tot}$ and Vgad showed prominent sensitivity to the $Vsc/Vtca_A$ ratio and not the other parameters tested. . Hence, variations in the scrambling rate introduce uncertainties that are larger than the scatter/noise in the data, emphasizing the importance of future studies to assess this parameter *in vivo*. Results from the sensitivity test employing CX data is shown in **Figure S10**, discussed in details below and proceeded by a paragraph detailing results from analysis of the other three brain regions.

Astroglial fraction of the aspartate pool (AspA)

The astroglial aspartate pool (AspA) is in rapid exchange with OAA, the product of the PC reaction, which might influence the rate of appearance of ^{13}C labeling in glutamine from [2-^{13}C]glucose (and Vpc) depending on the astroglial aspartate fraction, which is uncertain. Altering the AspA fraction from 1% to 40%, which is compatible with estimations from Ottersen et al.[6, 7] and rodent astroglia culture experiments[9, 16-18], had only a minor effect on the fitted value of Vpc of -2% to 2% from the nominal value (**Figure 6A**). Likewise, other fluxes showed little sensitivity to variations in the AspA fraction within this range, including the rates of GABA/glutamine and glutamate/glutamine cycling ($Vcyc_{GABAGln}$ and $Vcyc_{GluGln}$ respectively), the TCA cycle ($Vtca_{Tot}$), glutamate decarboxylase (Vgad), and glutamine synthetase (Vgln) which varied within -6% to +12% of the nominal value (see **Figure S10A**).

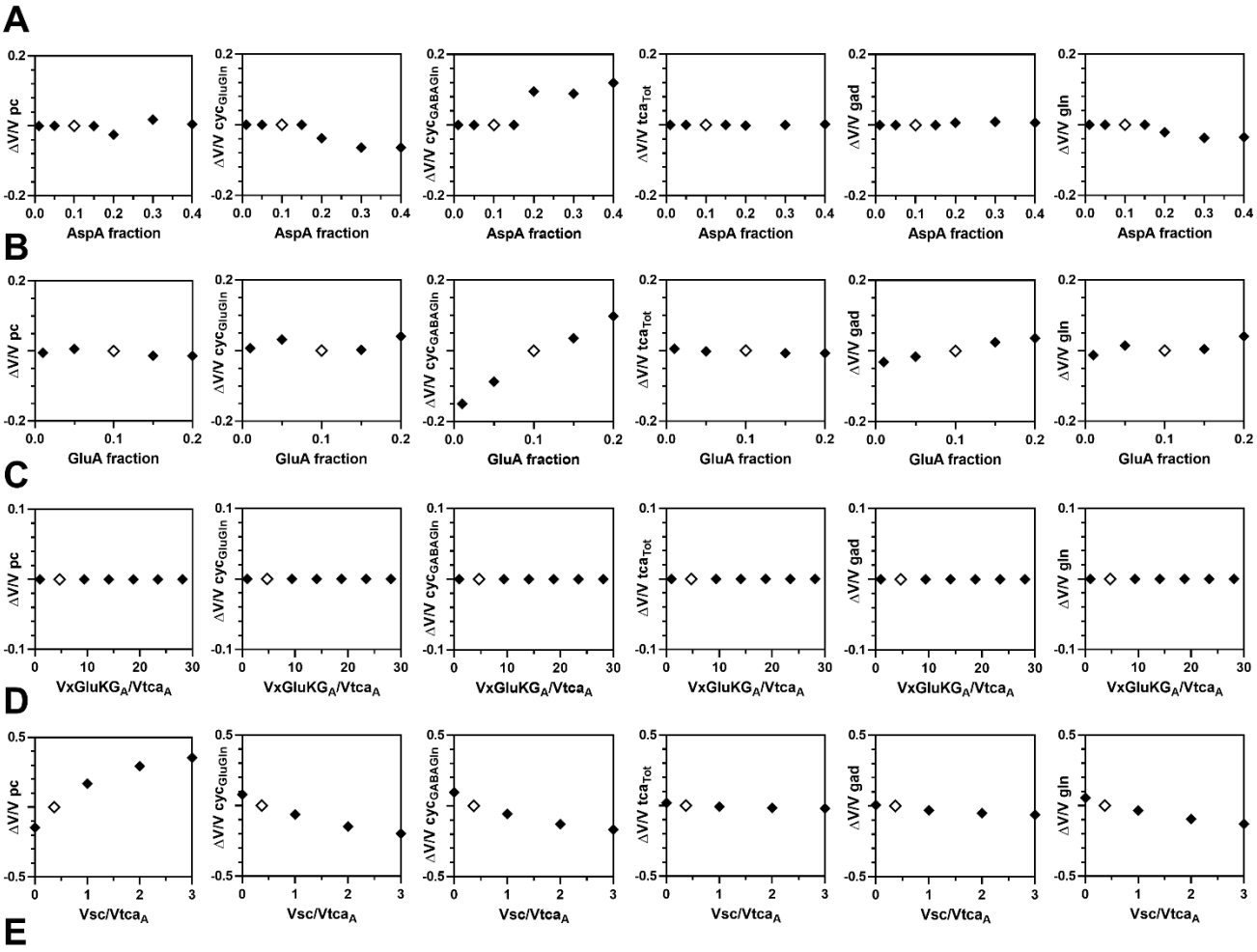

Figure S10. Results from local sensitivity analysis employing data from cerebral cortex. The local sensitivity of several metabolic rates to (A) the astroglial aspartate pool (AspA) fraction, (B) the astroglial glutamate pool (GluA) fraction, (C) the rate of exchange between glutamate and α-keotglutarate in the astroglia (Vx_{KGGluA}) relative to the rate of astrocytic tricarboxylic acid cycle ($Vtca_A$), and (D) the ratio between the rate of label cycling to fumatate (Vsc) and $Vtca_A$ was determined. ΔV/Vpc for $Vsc/Vtca_A$ equal to 5, 10, 15 and 20 were also tested (ΔV=0.4-0.5), but as they represent very unlikely scenarios, data was not included in the graph. Investigated rates included: Vpc, rate of pyruvate carboxylase (PC); $Vcyc_{GluGln}$, rate of glutamate/glutamine cycling; $Vcyc_{GABAGln}$, rate of GABA/glutamine cycling; V_{TCA}, rate of tricarboxylic acid (TCA) cycle; Vgad, rate of GABA synthesis catalyzed by glutamate decarboxylase (GAD); Vgln, rate of glutamine synthesis catalyzed by glutamine synthetase. ΔV, Change in rate from nominal value; White diamonds (◊), Nominal value of the parameter being tested; Black diamonds (♦), Parameter values tested.

Procedure for estimating the astrocytic aspartate pool (AspA) fraction in whole brain tissue from astroglia culture studies

The approximations listed in **Table S6** below employed Eq. S1 and are based on the assumption that the ratio of aspartate-to-glutamate concentrations in the astroglia culture ($AspA_{culture}/GluA_{culture}$) is equivalent to the ratio in astroglia in whole tissue *in vivo* ($AspA_{tissue}/GluA_{tissue}$), and that the astroglial glutamate pool in the whole tissue ($GluA_{tissue}$) equals 10% of the total ($GluTot_{tissue}$). The estimated AspA fractions range from 0.09 to 0.39, when based on the average values of $GluTot_{tissue}$ and $AspTot_{tissue}$ for cerebral cortex measured in the current study, 13.56 and 2.88 µmol/g wet weight, respectively.

Eq. S1
$$\mathbf{AspA\ fraction} = \frac{\mathbf{AspA_{tissue}}}{\mathbf{AspTot_{tissue}}} = \frac{\left(\frac{\mathbf{AspA_{culture}}}{\mathbf{GluA_{culture}}}\right) * \left(\frac{\mathbf{GluA_{tissue}}}{\mathbf{GluTot_{tissue}}}\right) * \mathbf{GluTot_{tissue}}}{\mathbf{AspTot_{tissue}}}$$

Table S6. Astroglial aspartate pool (AspA) fraction estimates

$AspA_{culture}/GluA_{culture}$	Astroglia culture preparation origin	Reference	AspA fraction
0.83	Mouse neo-cortex	[16]	0.39
0.21	Mouse cerebellum	[18]	0.10
0.33	Mouse neo-cortex	[17]	0.16
0.19	Rat cortex	[9]	0.09

Astroglial fraction of the glutamate pool (GluA)

As for the astroglial aspartate pool size, uncertainties exist concerning the distribution of the glutamate pool between neurons and astroglia. An astroglial glutamate pool (GluA) fraction ranging between 1.5% and 16% has been reported based on ^{13}C-labeling studies

in humans and rodents[4, 5, 8, 19]; hence our model was tested for its sensitivity to the size of this pool. For this analysis the GABAergic neuronal glutamate pool fraction was fixed at 0.02, while the astroglial glutamate pool fraction was varied between 0.01 and 0.20 at the expense of the glutamatergic neuronal pool. Vpc exhibited low sensitivity to the GluA fraction, varying only ±1% from the nominal value (**Figure 6B**). Likewise, $Vcyc_{GABAGln}$, $Vcyc_{GluGln}$, $Vtca_{Tot}$, Vgad, and Vgln varied modestly, from -15% to +10% from the nominal value (**Figure S10B**).

Astroglial αKG/Glu exchange rate (Vx_{GluKGA})

In the metabolic modeling the rate of label exchange between α-ketoglutarate (αKG) and glutamate (Glu) in neurons was treated as a free parameter, whereas for astroglia this parameter was constrained and the sensitivity of the fluxes to this parameter was tested. For values of the exchange rate in astroglia (Vx_{GluKGA}) between 1 and 30 times the astrocytic TCA cycle rate ($Vtca_A$), no effects on the determined fluxes were seen, i.e. variations from the nominal value of ≤ 0.001% (**Figure 6C** and **Figure S10C**).

Flux reversal and cycling between OAA and fumarate in astroglia

The rate of scrambling (Vsc), ^{13}C-labeling entering the TCA cycle *via* pyruvate carboxylase and then back-cycling from OAA to fumarate generating OAA-C3 from OAA-C2 and vice versa, was fixed based on the equilibration value for the ratio, $V_{fum}/(V_{fum}+V_g) = 0.27$, reported by Öz et al.[10], where V_{fum} is the back flux through fumarase and V_g is the astroglial PDH flux. Upon rearrangement, $V_{fum}/V_g = 0.37$, which is equivalent to $Vsc/Vtca_A$ in the terminology of the present study. The sensitivity of the

measured (iterated) rates to the Vsc/$Vtca_A$ ratio was assessed for values between 0 (no back cycling through fumarase) and 20. Not surprisingly, Vpc exhibited high sensitivity to this ratio when varied between 0 and 5, which led to values -15% to +42% from the nominal value (**Figure S10D**). For ratios ranging 5-20, by which Vsc is exceeding that of $Vtca_A$, almost no further change in the resulting Vpc was observed, i.e. +42-49% from nominal value. Whereas $Vtca_{Tot}$ and Vgad showed little sensitivity to the Vsc/$Vtca_A$ ratio, both $Vcyc_{GABAGln}$, $Vcyc_{GluGln}$ and Vgln was highly affected, varying -22% to +10% from the nominal value and likewise showing little change for ratios ranging from 5-20, during which variation from nominal values were at their largest (-8% to -31%; **Figure S10D**).

Local sensitivity analysis for data originating from CB, HP and ST

The same local sensitivity tests were conducted for data originating from CB, HP and ST. These confirmed that the value of Vpc was highly sensitive to Vsc/$Vtca_A$ ratio (-17 to +56% from nominal value) but relatively insensitive to deviations in the astroglial aspartate (AspA) and glutamate pool (GluA) fractions or astroglial Glu/αKG exchange rate (Vx_{GluKGA}), the latter deviating from the nominal values by < ±11% (data not shown). The exception was CB, which showed variation from the nominal value of -21% when the AspA fraction reached 0.4, although an aspartate pool this large *in vivo* is very unlikely. The same held true for the remaining rates evaluated ($Vcyc_{GABAGln}$, $Vcyc_{GluGln}$, $Vtca_{Tot}$, Vgad, and Vgln), varying at maximum -16% from the nominal value, with a few exceptions. These included the following striatal tests: For an AspA fraction of 0.01, $Vcyc_{GABAGln}$ varied -20%, for an AspA fraction of 0.3 or 0.4, $Vcyc_{GluGln}$ and Vgln varied

-20 to -30%; and hippocampal tests: For a GluA fraction of 0.15 and 0.20, $Vcyc_{GluGln}$ and Vgln varied -18 to -33% (data not shown). Finally, as observed for CX, the rates $Vcyc_{GABAGln}$, $Vcyc_{GluGln}$ and Vgln determined for CB, HP and ST showed high sensitivity to the Vsc/$Vtca_A$ ratio, whereas $Vtca_{Tot}$ and Vgad did not.

Supplementary results – The effect of astroglial dilution flux

We also evaluated the robustness of Vpc and certain other fluxes to the way in which astroglial glutamine dilution arose in the model. In the three-compartment model, the dilution in brain glutamine labeling is provided both by isotopic exchange with glutamine from blood ($Vdil_{Gln}$) and at the level of acetyl-CoA ($Vdil_{A\_in}$) by unidirectional influx and oxidation of unlabeled non-glucose substrates, such as acetate and fatty acids. $Vdil_{Gln}$ was calculated from the value of the ratio, $Vdil_{Gln}$/Vgln, which was iterated along with $Vdil_{A\_in}$. To assess the potential influence of the astroglial dilution (and where it originates) on the model-derived fluxes, the three-compartment model was refitted to the ^{13}C enrichment time course data with iteration of $Vdil_{A\_in}$ as before, but with $Vdil_{Gln}$ set to a constant value of 0.029 derived from the study of anesthetized mice by Bagga et al. (2014)[13] after adjustment for the blood concentration of glutamine in the present study, thus effectively placing the majority of the dilution as a flux of unlabeled carbon at the level of acetyl-CoA in the astrocytes. As expected, with $Vdil_{Gln}$ fixed to this low rate, the value of $Vdil_{A\_in}$ rose in an attempt to accommodate the dilution, increasing $Vtca_A$ ($Vtca_A$ = $Vpdh_A$ + $Vdil_{A\_in}$) by ~44% for CX (**Table S7**) and by a larger degree (165-191%) for the other brain regions (data not shown). In contrast to the large effect on glial oxidation

rates, the effect on Vpc was relatively small (-9% for CX to 33% in HP) and their spread across brain regions was similar ($Vdil_{Gln}$ fixed, 47% versus $Vdil_{Gln}$ iterated, 44%).

Table S7. Effects of astroglial OAA-to-fumarate cycling and dilution pathways on selected metabolic fluxes for cerebral cortex (CX) data fitted by the three-compartment model

		OAA-to-Fumarate Cycling Absent		**Astroglial glutamine Dilution**	
	Nominal Rate[1]	Vsc = 0		$Vdil_{Gln}$ = 0.029[2] *fixed*	
Fluxes	(µmol/g/min)	(µmol/g/min)	Δ(%)	(µmol/g/min)	Δ(%)
$Vpdh_A$	**0.126**	0.201	60	0.303	140
$Vtca_A$	**0.217**	0.313	44	0.519	139
Vpc	**0.106**	0.096	-9	0.105	-1
Vgln	**0.915**	0.804	-12	0.417	-54
Vsc	**0.080***	0		0.192	140
$Vdil_{A\_in}$	**0.090**	0.074	-18	0.231	157
$Vdil_{Gln}$	**0.247**	0.224	-9	0.029[2]	
$Vcyc_{(tot)}$	**0.809**	0.708	-12	0.313	-61
CMRglc(ox)	**0.802**	0.816	2	0.790	-1
$Vtca_{Tot}$	**1.80**	1.89	5	2.113	17
LSSD	1.432	1.419		1.613	

[1]The nominal values of the fluxes are expressed in units of µmol/g/min and reflect the best fit solutions of the three compartment metabolic model to the ^{13}C time course data with $Vsc/Vtca_A$ set to 0.37 based on the results of Öz et al. (2004)[30] (see the section "*Flux reversal and cycling between OAA and fumarate in astroglia"*) and with iteration of $Vdil_{Gln}$/Vgln and $Vdil_{A\_in}$ ($Vdil_{A\_out}$ = 0). [2]The value of $Vdil_{Gln}$ was set to 0.029 µmol/g/min based on the results of Bagga et al (2014) for $Vdil_{Gln}$ as determined under saturating blood glutamine levels (0.036 µmol/g/min for glutamine concentration ≥1 mM), and adjusting for the average blood glutamine concentration (0.80 mM) in the present study (=0.036 x 0.8mM/1 mM = 0.029 µmol/g/min). The asterisk (*) denotes assumed parameters used to generate the nominal values of the fluxes used for all other comparisons in this study. The flux definitions are given in **Table S1**. LSSD, Least Squares Standard Deviation, a global measure of the quality of fit of the model to the data.

As a consequence, the rate of anaplerosis *via* PC constituted a lesser fraction of astrocytic TCA cycle flux across the regions of 19% (CB) to 31% (CX), due mainly to the increase in dilution flux ($Vdil_{A\_in}$). Furthermore, anaplerosis as a fraction of $CMRglc_{(ox)}$ remained the same across the four regions (12-25% with VdilGln constrained versus 13-19% with

$Vdil_{Gln}$ as a free parameter). Compared to the relatively good fits of the model to the ^{13}C time course data for glutamine with $Vdil_{Gln}$ iterated (LSSD 1.432), the fits obtained with $Vdil_{Gln}$ constrained was poor (LSSD 1.613) with the curves substantially overshooting the data points.

Supplementary results – Correlation analysis

In the brain, one may find that PE in certain metabolites is lower than predicted from enrichment in other metabolites and plasma glucose enrichment. This is most likely due to dilution from non-labeled metabolites entering the brain and diluting fluxes are commonly introduced in metabolic models to accommodate this phenomenon. In our model, label dilution is provided through iterated rates introducing unlabeled glutamine from the blood to the brain ($Vdil_{Gln}$) or unspecified dilutions in the three cellular compartments−glutamatergic neurons ($Vdil_N$), GABAergic neuron (V_{dilG}) or astroglia ($Vdil_{A\_in}$)– potentially originating from metabolism of acetate[20-22], fatty acids[23] or ketone bodies[24]. Importantly, metabolic rates of interest may be sensitive to the dilution rates, as is true for any parameter in a metabolic model, constrained or not. To test the sensitivity to iterated dilutions, the correlation between measured metabolic rates and dilution rates were evaluated. An example of the complete 35-parameter heat map of correlation coefficients is given for CX data in **Figure S11**.

Whereas the correlation coefficient for Vpc and the dilution rates $Vdil_{Gln}$, $Vdil_{A\_in}$ and $Vdil_N$ ranged from 0.2 to 0.5 for all four brain regions, V_{dilG} and Vpc showed correlation coefficients of 0-0.02. This suggests that the glial and glutamatergic neuronal

dilutions have a higher impact on Vpc than the GABAergic neuronal dilution. The GABAergic rates $Vcyc_{GABAGln}$ and Vgad exhibited minimal correlations with the dilution rates having correlation coefficients of up to |0.3|. In contrast, $Vcyc_{GluGln}$, $Vtca_{Tot}$, and Vgln showed correlation coefficients of up to |0.7|, suggesting these rates were more sensitive to dilution. As expected, several rates correlated strongly due to one being calculated from the other or based on the same parameter. For example, $V_{max\_in} = V_{max\_out}$ or $Vgln = Vpc + Vcycle_{GluGln} + Vcycle_{GABAGln}$.

From the results of the correlation analysis, and comporting with expectations, across the four brain regions Vpc displayed weak to moderate correlations (R = |0.1| to |0.5|) with dilutional rates and moderate to strong correlations (R = |0.3| to |0.6|) with certain other rates, mainly reflecting flows into and out of the astrocytes and its TCA cycle. For highly correlated rates, reducing the statistical variance of one can often improve the determination of the other. Together with local sensitivity analysis, use of advanced statistical methods to better assess variances among the many interacting parameters (e.g., use of Global Sensitivity Analysis), and refinement of the measurement of label scrambling at the level of fumarate (and reflected by Vsc) can be expected to provide a more robust and accurate measurement of Vpc.

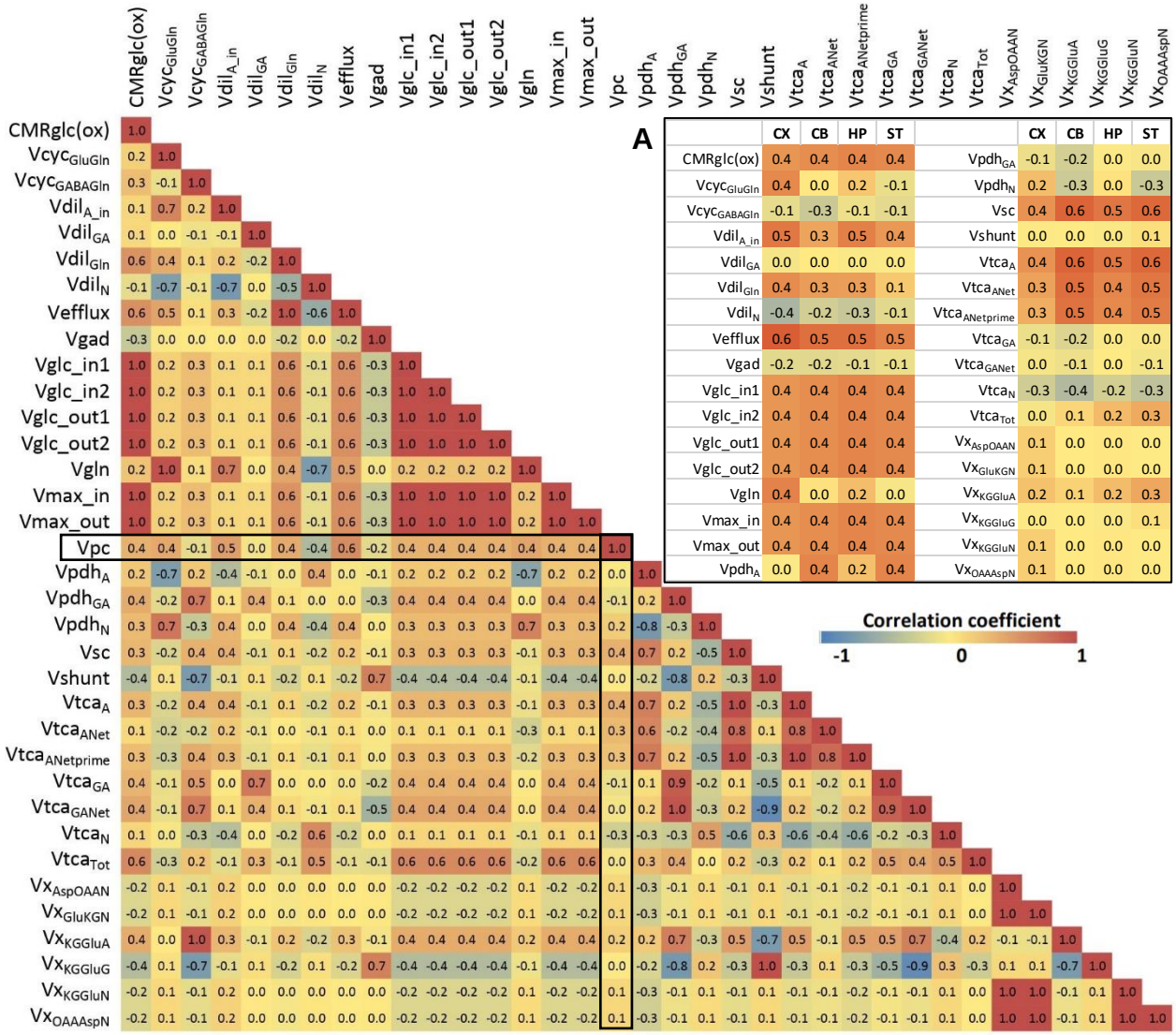

	CX	CB	HP	ST		CX	CB	HP	ST
CMRglc(ox)	0.4	0.4	0.4	0.4	$Vpdh_{GA}$	-0.1	-0.2	0.0	0.0
$Vcyc_{GluGln}$	0.4	0.0	0.2	-0.1	$Vpdh_{N}$	0.2	-0.3	0.0	-0.3
$Vcyc_{GABAGln}$	-0.1	-0.3	-0.1	-0.1	Vsc	0.4	0.6	0.5	0.6
$Vdil_{A\_in}$	0.5	0.3	0.5	0.4	Vshunt	0.0	0.0	0.0	0.1
$Vdil_{GA}$	0.0	0.0	0.0	0.0	$Vtca_{A}$	0.4	0.6	0.5	0.6
$Vdil_{Gln}$	0.4	0.3	0.3	0.1	$Vtca_{ANet}$	0.3	0.5	0.4	0.5
$Vdil_{N}$	-0.4	-0.2	-0.3	-0.1	$Vtca_{ANetprime}$	0.3	0.5	0.4	0.5
Vefflux	0.6	0.5	0.5	0.5	$Vtca_{GA}$	-0.1	-0.2	0.0	0.0
Vgad	-0.2	-0.2	-0.1	-0.1	$Vtca_{GANet}$	0.0	-0.1	0.0	-0.1
Vglc_in1	0.4	0.4	0.4	0.4	$Vtca_{N}$	-0.3	-0.4	-0.2	-0.3
Vglc_in2	0.4	0.4	0.4	0.4	$Vtca_{Tot}$	0.0	0.1	0.2	0.3
Vglc_out1	0.4	0.4	0.4	0.4	$Vx_{AspOAAN}$	0.1	0.0	0.0	0.0
Vglc_out2	0.4	0.4	0.4	0.4	Vx_{GluKGN}	0.1	0.0	0.0	0.0
Vgln	0.4	0.0	0.2	0.0	Vx_{KGGluA}	0.2	0.1	0.2	0.3
Vmax_in	0.4	0.4	0.4	0.4	Vx_{KGGluG}	0.0	0.0	0.0	0.1
Vmax_out	0.4	0.4	0.4	0.4	Vx_{KGGluN}	0.1	0.0	0.0	0.0
$Vpdh_{A}$	0.0	0.4	0.2	0.4	$Vx_{OAAAspN}$	0.1	0.0	0.0	0.0

Figure S11. Heat map illustrating correlations between 35 rates generated from the Monte-Carlo simulations of the cerebral cortex data, with an insert (A) showing correlations between Vpc and the remaining 34 rates across all four brain regions. Scale bar illustrates color code ranging from blue to red equal to Pearson product-moment correlation coefficients, R, ranging from -1 to 1. CX: cerebral cortex; CB: cerebellum; HP: hippocampus; ST: striatum. See **Table S1** for definitions and further details.

Supplementary results – Potential effects of hyperglycemia on the estimated rates

In our study, the glucose infusions raised blood glucose to hyperglycemic levels of 13 mM (from overnight fasting values of ~6 mM) during the 90 min period of the flux assessments, which could potentially have influenced the metabolic pathways and their estimated rates. Although we showed previously that brain glutamate and glutamine levels, high energy phosphates (phosphocreatine, nucleoside triphosphates) and intracellular pH (pH_i) were unaltered by the glucose infusion[25], the resulting hyperglycemia could potentially have influenced the metabolic pathways and their estimated rates. In studies of awake rats subjected to acute hyperglycemia (19 to 31 mM) over short time frames and measured using [6-^{14}C]glucose[26] or [2-^{14}C]-deoxyglucose (2DG) autoradiography[27], global and regional rates of glucose utilization were unchanged relative to normoglycemic controls, with exception of certain discrete regions (hypothalamus, globus pallidus, amygdala) that were increased. In contrast to an acute elevation of blood glucose, longer durations of hyperglycemia lasting days to weeks, as produced by streptozotocin treatment, may lead to altered rates of cerebral glucose utilization[27-31]. Thus, the short period of mild hyperglycemia would not be expected to alter the metabolic rates determined in our study.

Acute hyperglycemia reduces cerebral blood flow (CBF) in both anesthetized and awake rats[32, 33], although this occurs in the absence of changes in glucose utilization and energetics, which has been ascribed, in part, to hyperosmolarity effects on vascular

resistance. In awake rats, acute hyperglycemia (39 mM blood glucose) reduced regional CBF as measured by [^{14}C]iodoantipyrine autoradiography uniformly across multiple regions by 24%[33]. Taking note that CBF declines linearly by ~7% for each 10 mM increase in plasma glucose concentration up to 60 mM in awake rats[26], for the ~5 mM increase in plasma glucose produced in our study, CBF would be predicted to fall by only 4% over the course of the glucose infusion, a negligible amount.

Hyperglycemia may also alter the blood-to-brain transport of glucose by reducing glucose transporter 1 (GLUT1) expression[34], as seen with experimental diabetes with chronic but not acute elevation[35]. Reduced GLUT1 expression was seen in awake rats exposed to three weeks of chronic hyperglycemia (25 mM) but not after acute hyperglycemia[28], and in cerebral microvessels after one week of hyperglycemia[36]. Furthermore, in rats instrumented with microdialysis probes to sample cerebral extracellular fluid (ECF), the ECF-to-blood plasma glucose ratios were similar between normoglycemic, acute hyperglycemic and hyperglycemic-diabetic rats indicating the lack of adaptive effects of hyperglycemia on blood-brain-barrier glucose transport[37]. Finally, the brain glucose level measured in rats and humans by ^{1}H MRS of 1-2 mmol/L[1, 38-40] greatly exceeds the K_M for glucose (~45 μM) of hexokinase I[41], the level where brain glucose levels become limiting for glucose phosphorylation, and hyperglycemia increases brain glucose levels further with unchanging brain-to-plasma ratio of ~0.25[40]. Together, these observations suggest that brain glucose levels during hyperglycemia would not be limiting for metabolism.

Supplementary discussion – Limitations of the study

Metabolic rates derived from models depend on the data input and how the model is constructed, including parameter constraints and assumptions applied. We therefore tested the local sensitivity of determined fluxes to certain constrained parameters in the model, including the astrocytic aspartate and glutamate pool size, the Glu/αKG exchange rate in astroglia (Vx_{GluKGA}), and the extent of OAA-to-fumarate label scrambling (back-cycling). Of these parameters, Vpc (as well as other key rates investigated) proved relatively sensitive to Vsc; for Vsc/$Vtca_A$ exceeding 1, Vpc varied >25% from the nominal value. Öz et al.[10] included a dilution flux into glutamine (0.16 to 0.22 µmol/min/g) from the exchange between brain and blood, which was likewise implemented in the current model ($Vdil_{Gln}$). Glutamine transport through the blood-brain barrier is thought to be facilitated by the reversible system N transporter[42], and the close proximity of the astroglial end-feet to blood vessels suggest that astroglial rates may be more sensitive to this dilution. In the current study we observed significant plasma glutamine concentrations (0.8mM) and a significant $Vdil_{Gln}$ (0.24-0.31µmol/g/min) across regions. Determination of Vpc in the current metabolic model proved sensitive to $Vdil_{Gln}$ (rate-correlation analysis; r^2, 0.1-0.4), as well as other dilution rates in the astroglia ($Vdil_{A\_in}$; r^2, 0.3-0.5) and glutamatergic neuronal compartment ($Vdil_N$; r^2, 0.1-0.4). As these tests point toward the sensitivity of the determination of Vpc in particular to rates of label dilution and scrambling, improving knowledge of these parameters in future studies would improve the determination of Vpc in the current model.

Supplementary references

1. Mason GF, Behar KL, Rothman DL *et al.* NMR determination of intracerebral glucose concentration and transport kinetics in rat brain. *J Cereb Blood Flow Metab* 1992; 12(3)**:** 448-55.

2. Buschiazzo PM, Terrell EB, Regen DM. Sugar transport across the blood-brain barrier. *Am J Physiol* 1970; 219(5)**:** 1505-13.

3. Hawkins RA, Mans AM. Intermediary metabolism of carbohydrates and other fuels. In: *Metabolism in the Nervous System*. Springer US, 1983, pp 259-294.

4. Lanz B, Xin L, Millet P *et al.* In vivo quantification of neuro-glial metabolism and glial glutamate concentration using ^{1}H-[^{13}C] MRS at 14.1T. *J Neurochem* 2014; 128(1)**:** 125-39.

5. Lebon V, Petersen KF, Cline GW *et al.* Astroglial contribution to brain energy metabolism in humans revealed by 13C nuclear magnetic resonance spectroscopy: elucidation of the dominant pathway for neurotransmitter glutamate repletion and measurement of astrocytic oxidative metabolism. *J Neurosci* 2002; 22(5)**:** 1523-31.

6. Ottersen OP, Storm-Mathisen J. Glutamate- and GABA-containing neurons in the mouse and rat brain, as demonstrated with a new immunocytochemical technique. *J Comp Neurol* 1984; 229(3)**:** 374-92.

7. Ottersen OP, Storm-Mathisen J. Different neuronal localization of aspartate-like and glutamate-like immunoreactivities in the hippocampus of rat, guinea-pig and Senegalese baboon (Papio papio), with a note on the distribution of gamma-aminobutyrate. *Neuroscience* 1985; 16(3)**:** 589-606.

8. Tiwari V, Ambadipudi S, Patel AB. Glutamatergic and GABAergic TCA cycle and neurotransmitter cycling fluxes in different regions of mouse brain. *J Cereb Blood Flow Metab* 2013; 33(10)**:** 1523-31.

9. Zielińska M, Dąbrowska K, Hadera MG *et al.* System N transporters are critical for glutamine release and modulate metabolic fluxes of glucose and acetate in cultured cortical astrocytes: changes induced by ammonia. *J Neurochem* 2016; 136(2)**:** 329-38.

10. Öz G, Berkich DA, Henry PG *et al.* Neuroglial metabolism in the awake rat brain: CO_2 fixation increases with brain activity. *J Neurosci* 2004; 24(50)**:** 11273-9.

11. Chowdhury GM, Behar KL, Cho W *et al.* ^{1}H-[^{13}C]-nuclear magnetic resonance spectroscopy measures of ketamine's effect on amino acid neurotransmitter metabolism. *Biol Psychiatry* 2012; 71(11)**:** 1022-5.

12. Patel AB, Chowdhury GM, de Graaf RA *et al.* Cerebral pyruvate carboxylase flux is unaltered during bicuculline-seizures. *J Neurosci Res* 2005; 79(1-2)**:** 128-38.

13. Bagga P, Behar KL, Mason GF *et al.* Characterization of cerebral glutamine uptake from blood in the mouse brain: implications for metabolic modeling of ^{13}C NMR data. *J Cereb Blood Flow Metab* 2014; 34(10)**:** 1666-72.

14. Dadmarz M, vd Burg C, Milakofsky L *et al.* Effects of stress on amino acids and related compounds in various tissues of fasted rats. *Life Sci* 1998; 63(16)**:** 1485-91.

15. Wang J, Jiang L, Jiang Y *et al.* Regional metabolite levels and turnover in the awake rat brain under the influence of nicotine. *J Neurochem* 2010; 113(6)**:** 1447-58.

16. Amaral AI, Teixeira AP, Håkonsen BI *et al.* A comprehensive metabolic profile of cultured astrocytes using isotopic transient metabolic flux analysis and ^{13}C-labeled glucose. *Front Neuroenergetics* 2011; 3**:** 5.

17. Voss CM, Pajęcka K, Stridh MH *et al.* AMPK Activation Affects Glutamate Metabolism in Astrocytes. *Neurochem Res* 2015; 40(12)**:** 2431-42.

18. Waagepetersen HS, Sonnewald U, Larsson OM *et al.* A possible role of alanine for ammonia transfer between astrocytes and glutamatergic neurons. *J Neurochem* 2000; 75(2)**:** 471-9.

19. Patel AB, de Graaf RA, Rothman DL *et al.* Evaluation of cerebral acetate transport and metabolic rates in the rat brain in vivo using ^{1}H-[^{13}C]-NMR. *J Cereb Blood Flow Metab* 2010; 30(6)**:** 1200-13.

20. Badar-Goffer RS, Bachelard HS, Morris PG. Cerebral metabolism of acetate and glucose studied by ^{13}C-n.m.r. spectroscopy. A technique for investigating metabolic compartmentation in the brain. *Biochem J* 1990; 266(1)**:** 133-9.

21. Cerdan S, Künnecke B, Seelig J. Cerebral metabolism of [1,2-$^{13}C_2$]acetate as detected by in vivo and in vitro ^{13}C NMR. *J Biol Chem* 1990; 265(22)**:** 12916-26.

22. Deelchand DK, Shestov AA, Koski DM *et al.* Acetate transport and utilization in the rat brain. *J Neurochem* 2009; 109 Suppl 1(Suppl 1)**:** 46-54.

23. Ebert D, Haller RG, Walton ME. Energy contribution of octanoate to intact rat brain metabolism measured by ^{13}C nuclear magnetic resonance spectroscopy. *J Neurosci* 2003; 23(13)**:** 5928-35.

24. Künnecke B, Cerdan S, Seelig J. Cerebral metabolism of [1,2-$^{13}C_2$]glucose and [U-$^{13}C_4$]3-hydroxybutyrate in rat brain as detected by ^{13}C NMR spectroscopy. *NMR Biomed* 1993; 6(4)**:** 264-77.

25. Fitzpatrick SM, Hetherington HP, Behar KL *et al.* The flux from glucose to glutamate in the rat brain in vivo as determined by 1H-observed, ^{13}C-edited NMR spectroscopy. *J Cereb Blood Flow Metab* 1990; 10(2)**:** 170-9.

26. Duckrow RB, Beard DC, Brennan RW. Regional cerebral blood flow decreases during chronic and acute hyperglycemia. *Stroke* 1987; 18(1)**:** 52-8.

27. Orzi F, Lucignani G, Dow-Edwards D *et al.* Local cerebral glucose utilization in controlled graded levels of hyperglycemia in the conscious rat. *J Cereb Blood Flow Metab* 1988; 8(3)**:** 346-56.

28. Duelli R, Maurer MH, Staudt R *et al.* Increased cerebral glucose utilization and decreased glucose transporter Glut1 during chronic hyperglycemia in rat brain. *Brain Res* 2000; 858(2)**:** 338-47.

29. Mans AM, DeJoseph MR, Davis DW *et al.* Brain energy metabolism in streptozotocin-diabetes. *Biochem J* 1988; 249(1)**:** 57-62.

30. Pelligrino DA, Lipa MD, Albrecht RF. Regional blood-brain glucose transfer and glucose utilization in chronically hyperglycemic, diabetic rats following acute glycemic normalization. *J Cereb Blood Flow Metab* 1990; 10(6)**:** 774-80.

31. Jakobsen J, Nedergaard M, Aarslew-Jensen M *et al.* Regional brain glucose metabolism and blood flow in streptozocin-induced diabetic rats. *Diabetes* 1990; 39(4)**:** 437-40.

32. Duckrow RB. Decreased cerebral blood flow during acute hyperglycemia. *Brain Res* 1995; 703(1-2)**:** 145-50.

33. Duckrow RB, Beard DC, Brennan RW. Regional cerebral blood flow decreases during hyperglycemia. *Ann Neurol* 1985; 17(3)**:** 267-72.

34. Patching SG. Glucose Transporters at the Blood-Brain Barrier: Function, Regulation and Gateways for Drug Delivery. *Mol Neurobiol* 2017; 54(2)**:** 1046-1077.

35. Gjedde A, Crone C. Blood-brain glucose transfer: repression in chronic hyperglycemia. *Science* 1981; 214(4519)**:** 456-7.

36. Pardridge WM, Triguero D, Farrell CR. Downregulation of blood-brain barrier glucose transporter in experimental diabetes. *Diabetes* 1990; 39(9)**:** 1040-4.

37. Jacob RJ, Fan X, Evans ML *et al.* Brain glucose levels are elevated in chronically hyperglycemic diabetic rats: no evidence for protective adaptation by the blood brain barrier. *Metabolism* 2002; 51(12)**:** 1522-4.

38. Gruetter R, Novotny EJ, Boulware SD *et al.* Direct measurement of brain glucose concentrations in humans by ^{13}C NMR spectroscopy. *Proc Natl Acad Sci U S A* 1992; 89(3)**:** 1109-12.

39. Gruetter R, Ugurbil K, Seaquist ER. Steady-state cerebral glucose concentrations and transport in the human brain. *J Neurochem* 1998; 70(1)**:** 397-408.

40. de Graaf RA, Pan JW, Telang F *et al.* Differentiation of glucose transport in human brain gray and white matter. *J Cereb Blood Flow Metab* 2001; 21(5)**:** 483-92.

41. Grossbard L, Schimke RT. Multiple hexokinases of rat tissues. Purification and comparison of soluble forms. *J Biol Chem* 1966; 241(15)**:** 3546-60.

42. Bröer S, Brookes N. Transfer of glutamine between astrocytes and neurons. *J Neurochem* 2001; 77(3)**:** 705-19.